Energy Conversion and Management 237 (2021) 114082

Contents lists available at ScienceDirect

Energy Conversion and Management

journal homepage: www.elsevier.com/locate/enconman

Novel flow modulation method for R744 two-phase ejectors – Proof of concept, optimization and first experimental results

Paride Gullo [a,*], Michael Birkelund [b], Ekaterini E. Kriezi [b], Martin Ryhl Kærn [a]

[a] Technical University of Denmark (DTU), Department of Mechanical Engineering, Nils Koppels Allé, Building 403, 2800 Kgs., Lyngby, Denmark
[b] Danfoss A/S, Nordborgvej 81, 6430 Nordborg, Denmark

ARTICLE INFO

Keywords:
CO_2
Expansion work recovery
Refrigeration system
PWM
Transcritical system
Vapour-compression system

ABSTRACT

The cooling industry involves various essential applications, such as food preservation, medicine storage and air conditioning. However, its significant direct and indirect contribution to global warming is bound to increase in years to come, leading to the need for highly efficient cooling units using eco-friendly working fluids. Consequently, carbon dioxide (R744) is achieving resounding success as a refrigerant for various medium- and large-capacity applications, as some of the available expansion work is recovered with the aid of two-phase ejectors. However, its adoption is being limited for small-capacity solutions (e.g. condensing units) due to the current lack of a suitable flow modulation technique for two-phase ejectors installed in these units. Therefore, the goal of this work is to bridge this knowledge gap by formulating and experimentally proving an innovative flow control mechanism for two-phase ejectors, being based on the pulse-width modulation (PWM) of the refrigerant flow through the ejector. All the experimental evaluations were carried out at the compressor speed of 50 Hz, water temperature at the gas cooler inlet of 35 °C and R744 evaporating temperature of about −5 °C.

The first experimental data revealed that the high pressure can be controlled appropriately as well as varied from about 87 bar to 112 bar, demonstrating the effectiveness of the proposed technique. In addition, the effect of the muffler volume as well as the PWM period on the ejector and system performance were investigated. It was found that the influence of both the muffler volume and the PWM period was not significant. Compared to the solution employing the passive ejector (i.e. without flow modulation technique), the unit with the PWM ejector presented enhancements in coefficient of performance (COP) by more than 5% at the optimum operation conditions. It is worth mentioning that its today's available competitors, i.e. needle-based ejector and vortex-based ejector, feature COP enhancements by 2%–4% as contrasted with the passive ejector. As benchmarked to the standard unit (i.e. with flash gas by-pass valve and without ejector), the PWM ejector could improve the COP by more than 10% at the optimal running conditions. Also, the results obtained suggest that at present the proposed solution should operate with a PWM period of 2 s and no mufflers. Finally, the PWM ejector is characterized by low cost, simplicity, low vulnerability to clogging and no practical size or application constraints.

1. Introduction

The cooling demand is increasing considerably in step with world's temperatures as a consequence of global warming effect. Therefore, refrigeration and air conditioning (AC) solutions featuring high energy efficiency and ultra-low global warming potential (GWP) working fluids are considered essential to achieve Paris agreement targets. In a recent report, it was predicted that the energy efficiency enhancement of the cooling sector along with the transition to eco-friendly refrigerants could avoid an amount of greenhouse gas (GHG) emissions about equal to eight years of global GHG releases at 2018 levels over the next 40 years [62]. The need for energy saving in the cooling sector is even more exacerbated in small-capacity applications (e.g. condensing units). As an example, small-capacity refrigeration systems (i.e. condensing units) are responsible for 30%–60% of the total electricity required by small-format stores (i.e. grocery and convenience stores) [59]. In addition, grocery and convenience stores are about three times more energy intensive per sales area than large-format stores (e.g. hypermarkets) on an annual basis [59].

Thanks to its favourable environmental (i.e. negligible GWP, zero ozone depletion potential) and safety (i.e. non-toxic, non-flammable) properties, carbon dioxide is a leading option as a refrigerant (R744) for various cooling applications, such as chillers [51]), supermarkets [13],

* Corresponding authors.
E-mail address: parigul@mek.dtu.dk (P. Gullo).

https://doi.org/10.1016/j.enconman.2021.114082
Received 8 January 2021; Accepted 17 March 2021

Nomenclature

Symbols and abbreviations

AC	Air conditioning
CFD	Computational fluid dynamics
COP	Coefficient of Performance [–]
EES	Engineering equation solver
EG	Ethylene glycol-water (35/65 %) mixture
GHG	Greenhouse gas
GWP	Global Warming Potential [$kg_{CO2,equ}$Â·$kg^{-1}_{refrigerant}$]
h	Enthalpy per unit mass [kJ·kg^{-1}]
HFC	Hydrofluorocarbon
HVAC&R	Heating, ventilation, air conditioning and refrigeration
IHX	Internal heat exchanger
$\dot{m}$	Mass flow rate [kg·s^{-1}]
MSV	Motive solenoid valve
OD	Opening degree [%]
P	Pressure [bar]
PAG	Polyalkylene glycol
PWM	Pulse-width modulation
$\dot{Q}$	Cooling capacity [kW]
s	Entropy per unit mass [kJ·kg^{-1}·K^{-1}]
SLHX	Suction line heat exchanger
t	Temperature [°C]
T	Temperature [K]
$\dot{V}$	Volume flow rate [m^3·s^{-1}]
$\dot{W}$	Power [kW]

Subscripts and superscripts

compr	Compressor
diff	Diffuser
eg	Ethylene glycol-water (35/65 %) mixture
evap	Evaporator
gc	Gas cooler
in	Inlet
m	Mass
mn	Motive nozzle
out	Outlet
sn	Suction nozzle

Greek symbols

Δ	Variation
η	Efficiency [–]
ρ	Density [kg·m^{-3}]
Φ	Entrainment ratio [–]

trains [44], light commercial refrigerators [46], air conditioners [6]and cars [64], in which hydrofluorocarbon (HFC)-based vapour-compression systems are by far predominant. However, the typical decline in overall system efficiency with rise in heat sink temperature is particularly marked for R744 due to the occurrence of transcritical running modes [5]. For the purpose of surmounting this disadvantage, many solutions for transcritical R744 vapour-compression systems, such as parallel compression [58,23], overfed evaporators [28,22], dedicated mechanical subcooling [52,24], system integration [21,20], gas cooler effectiveness enhancement [60,61], direct space cooling [17], cold thermal energy storages [50,33], have been proposed. Also, the significant heat recovery opportunity attributable to transcritical R744 units [50] promotes energy saving [49,55], better environmental performance [11]and promising payback times [53].

Among the aforementioned solutions, two-phase ejectors for expansion work recovery are perceived to be the most promising measure to enhance the performance of transcritical R744 vapour-compression units [27,54]. Elbel and Lawrence [7] evaluated COP improvements between 10% and 30% thanks to two-phase ejectors for transcritical R744 systems at design operation conditions. As an example, Nakagawa et al. [47] experimentally measured a maximum COP enhancement of 27% over a standard transcritical R744 system at design running modes. However, the benefits deriving from two-phase ejectors are lost at off-design operation conditions as an appropriate flow modulation strategy along with an effective expansion work recovery is not implemented [35,16,65]. It is worth remarking that the majority of vapour-compression systems works most of the time at off-design operations, regardless their application as well as their scale. Also, transcritical R744 vapour-compression units are characterized by an optimal heat rejection pressure maximizing the COP with respect to R744 temperature at the gas cooler outlet as soon as the transcritical running modes occur [43,34]. Consequently, it is of fundamental importance for transcritical R744 units that their high pressure is accurately controlled. This duty is fulfilled by either the high pressure valve (in standard transcritical R744 systems) or by the two-phase ejector. As a reference, Nakagawa et al. [47] also experienced COP penalizations between 34% and 82% as well as 12% degradation in ejector efficiency at off design conditions (i.e. gas cooler pressure between 12.5 bar and 15.0 bar below optimal value).

1.1. Ejector flow modulation techniques

To the best of the authors' knowledge, three flow modulation techniques are currently available, i.e. needle-based ejector mechanism [8,42], multi-ejector concept [26,18] and vortex ejector-based strategy [65].

As for needle-based ejectors, their motive nozzle efficiency was found to decrease with reduction in the motive nozzle throat area, while their motive nozzle throat area and the outdoor temperature were found to affect their suction nozzle efficiency for refrigeration cycles [39]. The experimental investigation by Liu and Groll [41] brought to light ejector motive nozzle, suction nozzle and mixing section efficiencies of 0.50–0.93, 0.37–0.90 and 0.50–1.00, respectively. Liu and Groll [40] experimentally assessed that the use of the needle-based ejector leads to more significant COP improvements with decrease in motive nozzle throat diameter and compressor frequency as well as with rise in outdoor temperature for air conditioners. The experimental work by Liu et al. [38] showed that a transcritical R744 air conditioner equipped with a needle-based ejector offers enhancements in COP and cooling capacity by about 30.7% and 32.1% compared to the conventional unit, respectively. A transcritical R744 vapour-compression system for concurrent cooling and heating and outfitted with a needle-based ejector was found to have 71.4% higher COP, whereas the system capacity was found to be 21.3% lower [37]. He et al. [31] computed 5%–11% lower mass entrainment ratio (ratio of suction nozzle mass flow rate to motive nozzle mass flow rate) and similar exergy efficiency compared to the ejector without flow modulation. The experimental work by Xu et al. [63] revealed needle-based ejector efficiencies between 0.20 and 0.30 in heat pump applications. Although this technique has no constraints in terms of application size, it is significant vulnerable to clogging [35,65], being particular detriment to small-capacity applications. In addition, this technique is complicated and costly [35,65]as well as its reliability is weakened by the presence of moving parts [2]and the absence of available field data [12].

As regards the multi-ejector block, it was firstly studied by Hafner et al. [26], who concluded that COP values in cooling mode can be augmented by 17% in Athens (Greece), 16% in Frankfurt (Germany) and 5% in Trondheim (Norway). Banasiak et al. [1] mapped the efficiencies of the ejectors installed in a multi-ejector block for supermarket

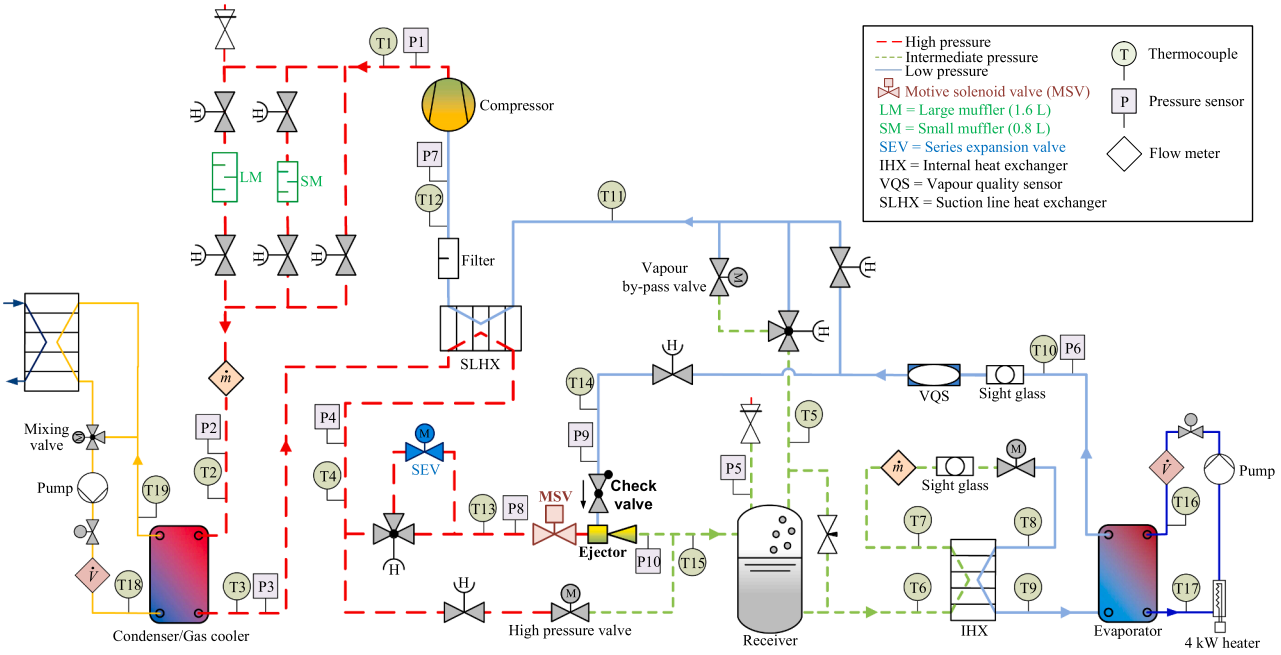

Fig. 1. Schematic of the experimental facility.

refrigeration applications. The authors observed that the proposed expansion work recovery device is capable of appropriately controlling the high pressure as well as ejector efficiencies above 0.30 over a wide range of the evaluated running modes were measured. The experimental investigation by Bodys et al. [3] brought to light that the use of the multi-ejector block does not result in unstable performance in supermarket applications. Haida et al. [30] experimentally revealed that the multi-ejector module improves the COP by 7% compared to parallel compression. Also, ejector efficiencies up to 0.33 were found with respect to the pressure lift (pressure difference between diffuser outlet and suction inlet) and the motive and suction conditions. Schönenberger [56] observed an energy saving between 15% and 25% depending on the heating need, application and weather context as a consequence of the use of the multi-ejector concept compared to parallel compression. The field data presented by Hafner et al. [25] proved that the use of the multi-ejector concept results in energy consumption decrements ranging from 15% to 30% in comparison with parallel compression at outdoor temperatures between 22 °C and 35 °C. Palacz et al. [48] optimized the mixing section shape of three ejectors mounted in the multi-ejector module by implementing a computational fluid dynamics (CFD) analysis. The numerical work by Bodys et al. [4] revealed that the benefits from swirl flow at the inlet of the motive and suction nozzles are negligible in terms of mass entrainment ratio enhancement. The performance of four ejectors of the multi-ejector block was mapped by Haida et al. [29] for refrigeration and air conditioning supermarket applications. As for heat pump water heaters, Boccardi et al. [2] experimentally showed the existence of an optimum multi-ejector configuration. On the one hand, the multi-ejector concept is leading transcritical R744 refrigeration systems to flourish in supermarkets [19], even in hot climates [57]. On the other hand, with respect to small-capacity applications this flow modulation mechanism is too complex [7], costly [45,65]and limited by manufacturing sizes.

Finally, the vortex ejector-based technique was recently implemented by Zhu and Elbel [65], being simpler, less vulnerable to clogging as well as potentially cheaper than the needle-based ejector mechanism. However, at present the vortex ejectors perform similarly to or slightly worse than the latter [65].

1.2. Scope

The literature review has revealed the need to formulate new flow modulation strategies for two-phase ejectors installed in small-capacity transcritical R744 vapour-compression units. Therefore, the target of this work is to bridge this knowledge gap by establishing the experimental evidence as well as by presenting the first experimental results related to an innovative flow control mechanism for two-phase ejectors in a small-capacity transcritical R744 vapour-compression system. The new flow modulation technique is based on the pulse-width modulation (PWM) of R744 flow through the ejector. The investigation has been carried out at the compressor speed of 50 Hz, water temperature at the gas cooler inlet ($t_{water,gc\ in}$) of 35 °C, ethylene glycol–water (35/65%) mixture (EG) temperature at the evaporator inlet ($t_{eg,evap\ in}$) of 5 °C, resulting in R744 evaporating temperature (t_{evap}) of about −5 °C (typical value for condensing units), and degree of superheating ($\Delta T_{superheating}$) of 8 K. Besides the proof of the PWM concept, the influence of the PWM period as well as that of the presence and volume of mufflers on the PWM ejector and overall system performance have been investigated. Furthermore, the performance of the PWM ejector has been compared to that of the passive ejector (i.e. ejector without flow modulation technique) as well as to that of the standard solution (i.e. with flash gas by-pass valve and without ejector).

The work is structured as follows: the experimental facility, the PWM concept, the test procedure and the uncertainty analysis are described in Section 2, while the results are presented and discussed in Section 3. Finally, the conclusions and future developments are summed up in Section 4.

2. Methodology

2.1. PWM working principle

The PWM concept has been widely used in expansion valves to control the superheating degree in various heating, ventilation, air conditioning and refrigeration (HVAC&R) applications. As for expansion valves, this methodology operates as follows:

Table 1
Primary geometry parameters of the employed two-phase ejector.

Parameter	Value	Unit of measurement
Motive nozzle inlet diameter	3.80	mm
Motive nozzle throat diameter	0.71	mm
Motive nozzle outlet diameter	0.79	mm
Motive nozzle converging angle	30.00	°
Motive nozzle diverging angle	2.00	°
Diffuser outlet diameter	7.30	mm
Diffuser angle	5.00	°

- within a time period (i.e. PWM period or cycle time) of commonly 3–6 s, a voltage signal from the controller is transmitted to and removed from the valve coil, leading respectively to the opening and closing of the valve coil (i.e. to the flow of the refrigerant through the expansion valve or not);
- the appropriate refrigerant flow for matching the required cooling capacity is provided by varying the relation between the opening and closing time of the valve coil.

This means that, if the required cooling duty is 70% of the full capacity, the valve coil will be open for 70% of the PWM period and closed for the following 30% of the PWM period. As 30% of the full duty is needed, the valve coil will be open for 30% of the PWM period and closed for the following 70% of the PWM period. Therefore, the valve coil provides the full capacity by remaining open over the whole PWM period. The same concept was applied to the solenoid valve mounted upstream of the ejector motive nozzle (indicated as MSV in Fig. 1) for the purpose of controlling the on/off state of the expansion work recovery device and thus modulate the R744 flow through the ejector. Therefore, the PWM period of the ejector was optimized by investigating three different values, i.e. 1 s, 2 s and 3 s. In fact, on the one hand, the PWM period cannot be too short to avoid deteriorating system stability and cause spurious system level pressure oscillations. On the other hand, the PWM period needs to be faster than that of an expansion valve without compromising the lifetime of the valve.

2.2. Experimental facility

The employed experimental facility (Fig. 1) can be used in either ejector mode or standard mode (i.e. with flash gas by-pass valve and without ejector) [32]. The test rig is equipped with an R744 transcritical semi-hermetic reciprocating compressor with a displacement of 1.12 $m^3 \cdot h^{-1}$ at 1450 rpm and a power analyser, being installed between the drive and the compressor. Consequently, the losses due to the variable speed drive in the readings were not considered. Brazed plate heat exchangers were employed as the evaporator (0.492 m^2 of heat transfer area) and the condenser/gas cooler (0.328 m^2 of heat transfer area). The experimental apparatus also presents a suction line heat exchanger (SLHX), being 50 cm stainless steel tubes tin-soldered together. The employed two-phase ejector, whose main geometry parameters are summarized in Table 1, was a 2 kW low pressure lift device. Stepper-motor expansion valves were used for controlling the intermediate pressure (in standard mode), the superheating degree of the evaporator and the high pressure (in standard mode). The refrigerant discharged by the compressor could flow through: (i) the pipe leading to a small muffler (volume: 0.8 L), (ii) the pipe bringing to a large muffler (volume: 1.6 L), (iii) the pipe without mufflers or (iv) two or more of them simultaneously. The path taken by R744 leaving the compressor could be imposed with the aid of manually active valves. The mufflers were located between the compressor and the condenser/gas cooler to avoid trapping high density gas/liquid, resulting in refrigerant charge issues. The purpose of the buffers was to potentially attenuate the pressure oscillations generated by the MSV opening and closing (fluid hammer effect) through the high pressure side (see Section 3.1). Polyalkylene glycol (PAG) oil was used and its return to the compressor was guaranteed by means of a by-pass line from the liquid outlet of the separator to the vapour outlet (compressor suction line). A metering valve was included in the oil return line. The test rig also presents a liquid level sensor as well as a 3 L receiver with two sight glasses (i.e. at top and bottom). A refrigerant charge of about 45% of full capacity (measured at steady state in ejector mode) was considered in all the tests. This corresponded to an R744 level at the bottom sight glass, meaning that enough R744 could be visualized in the receiver during the whole experimental campaign. The experimental setup is fitted with two secondary working fluid loops. One loop is employed for handling the heat removed in the evaporator with the aid of EG, whereas the other is used for rejecting the heat in the condenser/gas cooler with the aid of distilled water. Inlet temperature of water flowing through the condenser/gas cooler and that of EG flowing through the evaporator were respectively controlled by employing a 3-way mixing valve and a 4 kW electric heater, whereas the flows were controlled with the aid of 2-way valves. Similarly to the PWM ejector, the electrical heater was controlled by PWM effect. Ten pressure gauges (all for R744), nineteen temperatures sensors (fifteen for R744, two for distilled water, two for EG), two mass flow meters for R744 and one volume flow meter for each secondary working fluid (one for water and the other for EG), whose accuracies and calibration range are listed in Table 2, were mounted. One out of two R744 mass flow meters was installed between the mufflers and the condenser/gas cooler. An internal heat exchanger (IHX), i.e. 100 cm hair-pinned stainless steel tubes tin-soldered together, was adopted upstream of the evaporator expansion valve to guarantee the absence of vapour at the inlet of the other R744 mass flow meter on the intermediate pressure side. Pressure sensors associated with the motive nozzle, suction nozzle and diffuser pressures were installed directly on the ejector housing. Also, pressures and flow rates were logged respectively at 1000 Hz and every 0.01 s, whereas temperatures were acquired every 0.10 s. Finally, the power analyser as well as all the temperature and pressure sensors were recalibrated accurately before the experimental campaign implementation.

Table 2
Accuracies and calibration range of the measurement devices.

Measured parameter	Measurement device	Calibration range	Unit of measurement	Uncertainty
Temperature	T-type thermocouples	−20.00 to−145.00	°C	±0.13 °C
R744 pressure	Pressure gauges	0.00 to 120.00	bar	±0.13% of full scale
R744 mass flow rate on high pressure side	Coriolis flow meter	1.03 to 5.17	$kg \cdot min^{-1}$	±0.25% of reading
R744 mass flow rate on intermediate pressure side	Coriolis flow meter	1.03 to 5.17	$kg \cdot min^{-1}$	±0.10% of reading
Water volumetric flow rate in gas cooler	Magnetic flow meter	0.50 to 17.30	$l \cdot min^{-1}$	±0.40% of reading
EG volumetric flow rate in evaporator	Turbine flow meter	0.50 to 15.00	$l \cdot min^{-1}$	0.74% of full scale
Compressor power input	Power meter	0.00 to 6.00	kW	0.10% of reading

2.3. Test procedure

The investigation was implemented at the compressor speed of 50 Hz (i.e. nominal value), $t_{water,gc\ in} = 35.0\ °C \pm 0.5\ °C$, $t_{evap} = -5.0\ °C \pm 0.5\ °C$ (i.e. $t_{eg,evap\ in} = 5.0\ °C \pm 0.5\ °C$) to simulate condensing units, and $\Delta T_{superheating} = 8.0\ K \pm 0.5\ K$. The selected $t_{water,gc\ in}$ is a typical value at which two-phase ejectors are designed [35]. The water mass flow rate

Table 3
Experimental uncertainties of the calculated parameters.

Parameter	Uncertainty
COP [-]	±0.063
$\dot{Q}_{eg,evap}$ [kW]	±0.083
$\eta_{ejector}$ [-]	±0.003
P_{lift} [bar]	±0.026
Φ_m [-]	±0.003

and EG mass flow rate were set to 0.0918 kg·s^{-1} ± 0.0044 kg·s^{-1} and 0.1152 kg·s^{-1} ± 0.0004 kg·s^{-1}, respectively. Steady states were obtained as all the temperatures were recorded within ± 0.2 °C for 60 s. The data were logged for 5 consecutive minutes and averaged over the collection period. The repeatability of the collected data was evaluated to be within 2%. Minilog was mainly used to control/monitor the test rig, whereas data acquisition was performed by using LabView 2016 and National Instruments cDAQ modules.

The COP was computed by considering the heat from the EG side and the measured compressor power (Eq. (1)).

$$COP = \frac{\dot{Q}_{eg,evap}}{\dot{W}_{compr}} = \frac{\dot{V}_{eg} \cdot \rho_{eg} \cdot \left(h_{eg,evapin} - h_{eg,evapout}\right)}{\dot{W}_{compr}} \quad (1)$$

The mass entrainment ratio and the pressure lift were calculated via Eqs. (2) and (3), respectively.

$$\Phi_m = \frac{\dot{m}_{sn}}{\dot{m}_{mn}} \quad (2)$$

$$P_{lift} = P_{diffout} - P_{snin} \quad 3)$$

Also, the definition of ejector efficiency formulated by Elbel and Hrnjak [8] (Eq. (4)) was employed for investigating the performance of the expansion work recovery device.

$$\eta_{ejector} = \Phi_m \cdot \frac{h\left(P_{diffout}, s_{snin}\right) - h_{snin}}{h_{mnin} - h\left(P_{diffout}, s_{mnin}\right)} \quad (4)$$

2.4. Uncertainty analysis

The uncertainty analysis, whose results are summarized in Table 3, was carried out by employing Engineering Equation Solver (EES) [9]. The thermo-physical properties of R744, water and EG were obtained from REFPROP [36] during the data reduction process. Finally, it was

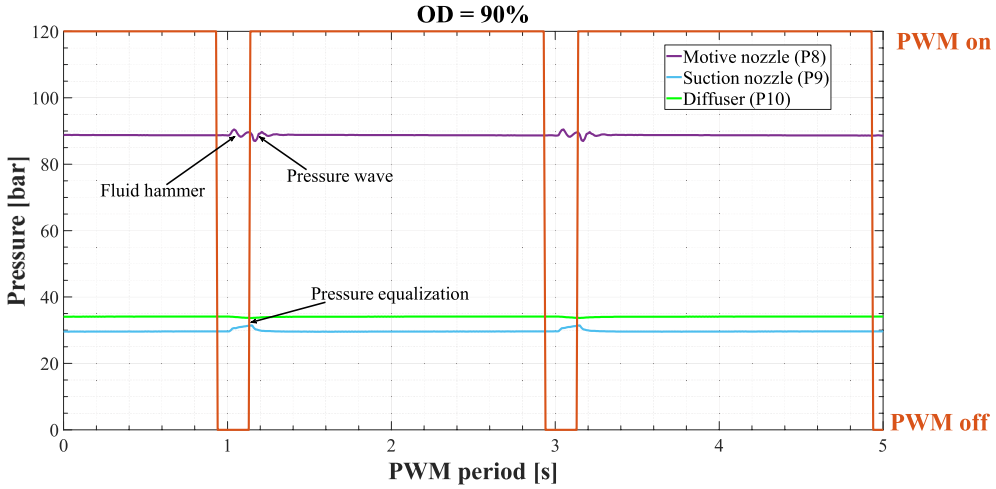

Fig. 2a. Influence of the MSV opening degree (OD) of 90% on the motive nozzle, suction nozzle and diffuser outlet pressures of the ejector (compressor speed = 50 Hz, $t_{water,gc\ in}$ = 35 °C, $t_{eg,evap\ in}$ = 5 °C, $\Delta T_{superheating}$ = 8 K, PWM period = 2 s).

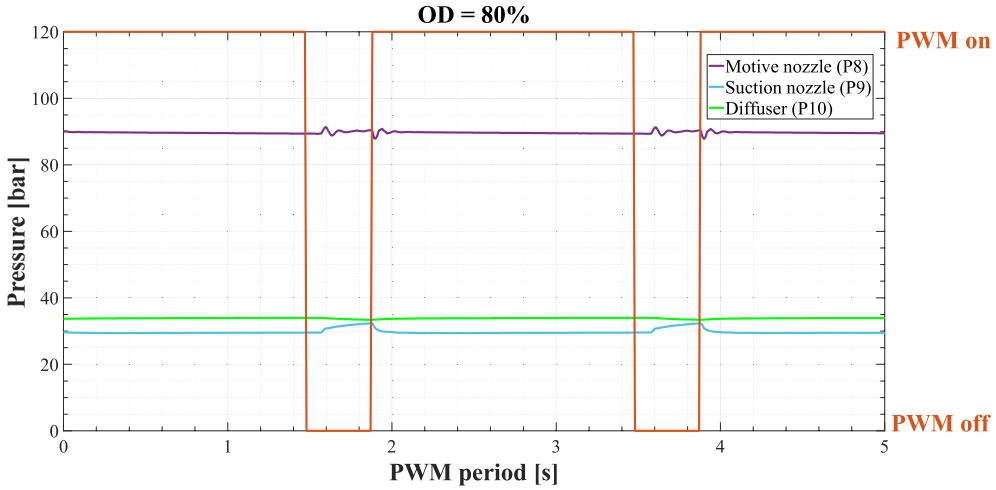

Fig. 2b. Influence of the MSV opening degree (OD) of 80% on the motive nozzle, suction nozzle and diffuser outlet pressures of the ejector (compressor speed = 50 Hz, $t_{water,gc\ in}$ = 35 °C, $t_{eg,evap\ in}$ = 5 °C, $\Delta T_{superheating}$ = 8 K, PWM period = 2 s).

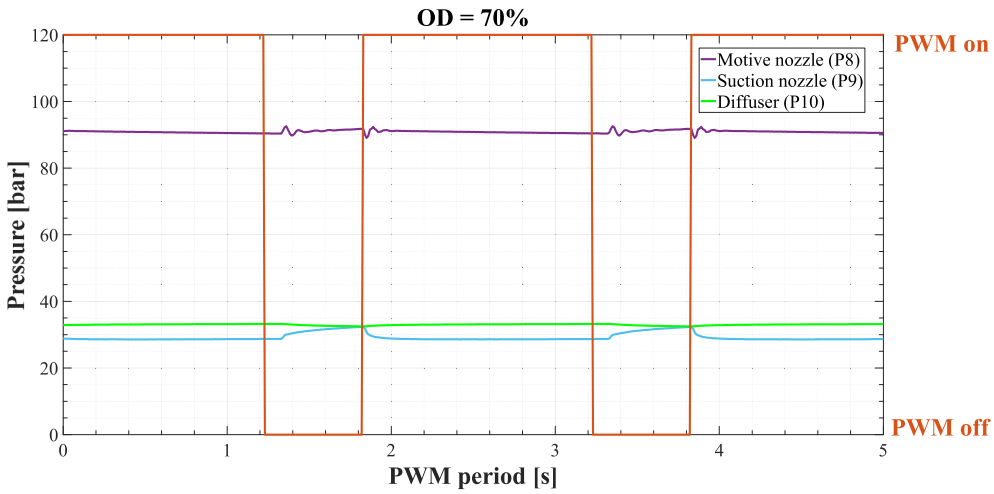

Fig. 2c. Influence of the MSV opening degree (OD) of 70% on the motive nozzle, suction nozzle and diffuser outlet pressures of the ejector (compressor speed = 50 Hz, $t_{water,gc\ in}$ = 35 °C, $t_{eg,evap\ in}$ = 5 °C, $\Delta T_{superheating}$ = 8 K, PWM period = 2 s).

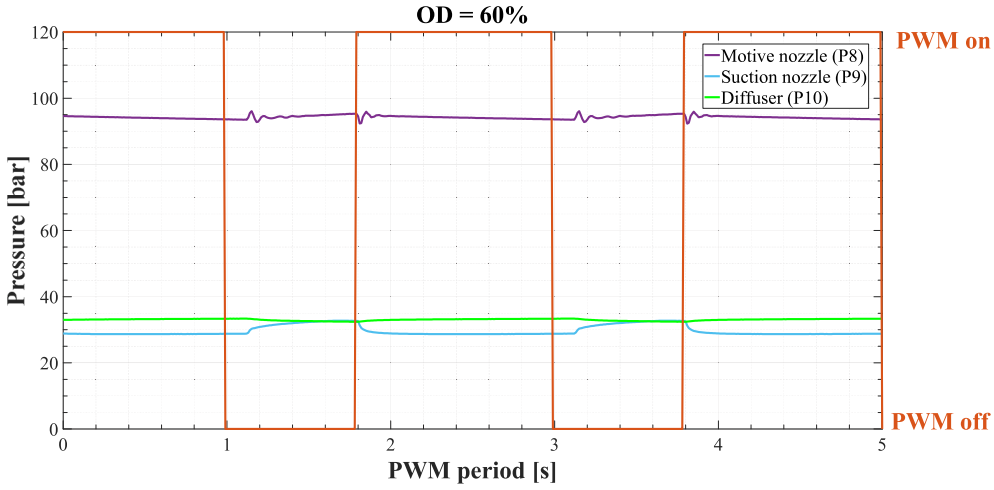

Fig. 2d. Influence of the MSV opening degree (OD) of 60% on the motive nozzle, suction nozzle and diffuser outlet pressures of the ejector (compressor speed = 50 Hz, $t_{water,gc\ in}$ = 35 °C, $t_{eg,evap\ in}$ = 5 °C, $\Delta T_{superheating}$ = 8 K, PWM period = 2 s).

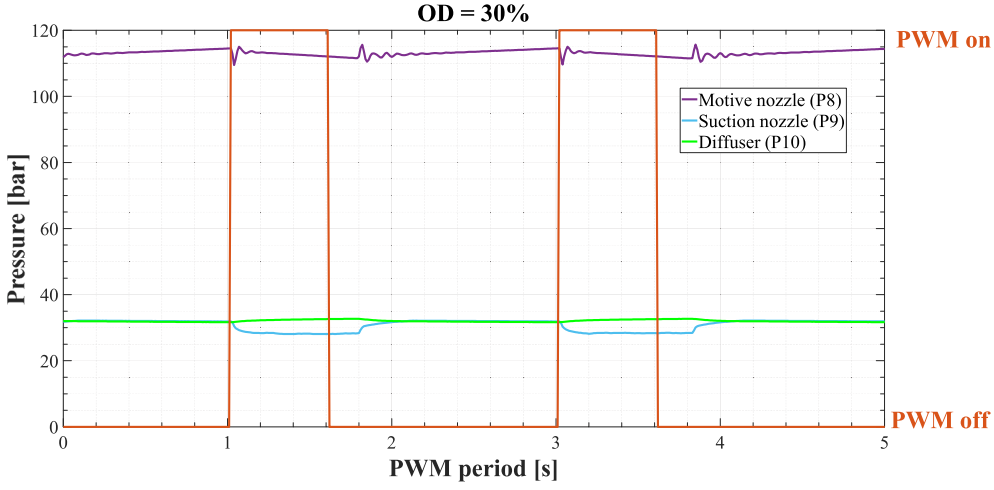

Fig. 2e. Influence of the MSV opening degree (OD) of 30% on the motive nozzle, suction nozzle and diffuser outlet pressures of the ejector (compressor speed = 50 Hz, $t_{water,gc\ in}$ = 35 °C, $t_{eg,evap\ in}$ = 5 °C, $\Delta T_{superheating}$ = 8 K, PWM period = 2 s).

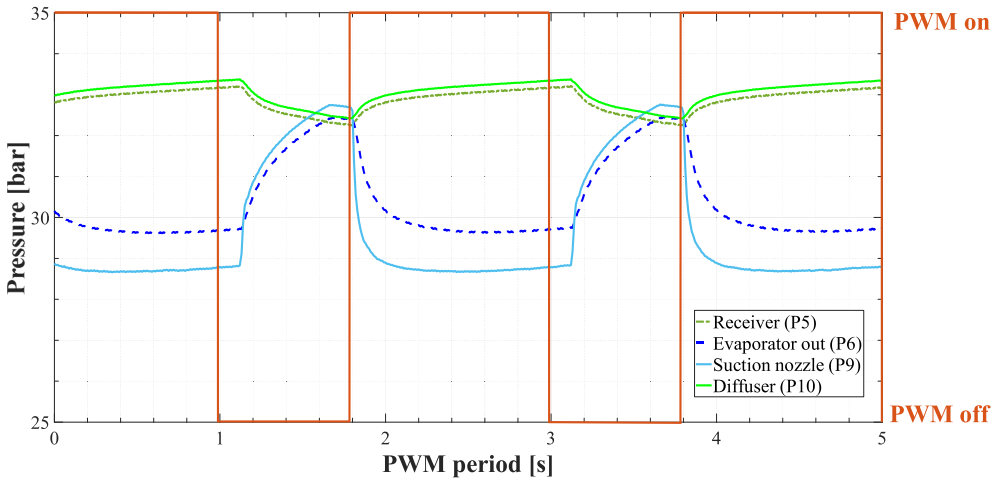

Fig. 2f. Detail of the PWM transients in terms of receiver, evaporator outlet, suction nozzle and diffuser outlet pressures of the ejector (compressor speed = 50 Hz, $t_{water,gc\ in}$ = 35 °C, $t_{eg,evap\ in}$ = 5 °C, $\Delta T_{superheating}$ = 8 K, PWM period = 2 s, OD = 60%).

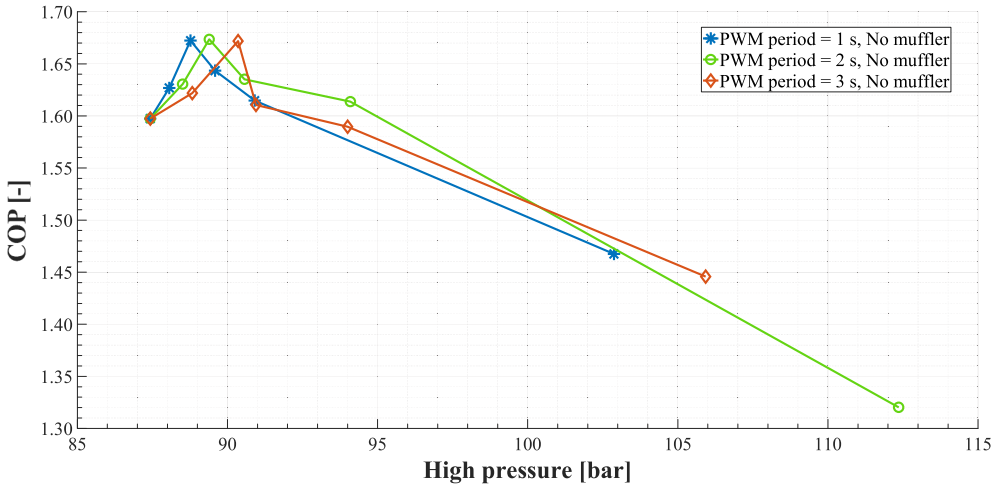

Fig. 3a. COP as a function of high pressure and PWM period (compressor speed = 50 Hz, $t_{water,gc\ in}$ = 35 °C, $t_{eg,evap\ in}$ = 5 °C, $\Delta T_{superheating}$ = 8 K).

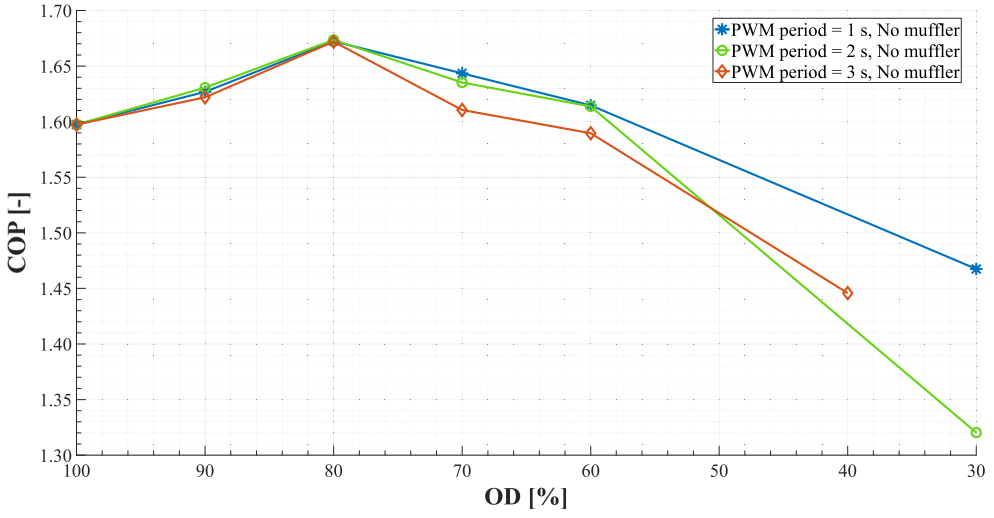

Fig. 3b. COP as a function of MSV opening degree (OD) and PWM period (compressor speed = 50 Hz, $t_{water,gc\ in}$ = 35 °C, $t_{eg,evap\ in}$ = 5 °C, $\Delta T_{superheating}$ = 8 K).

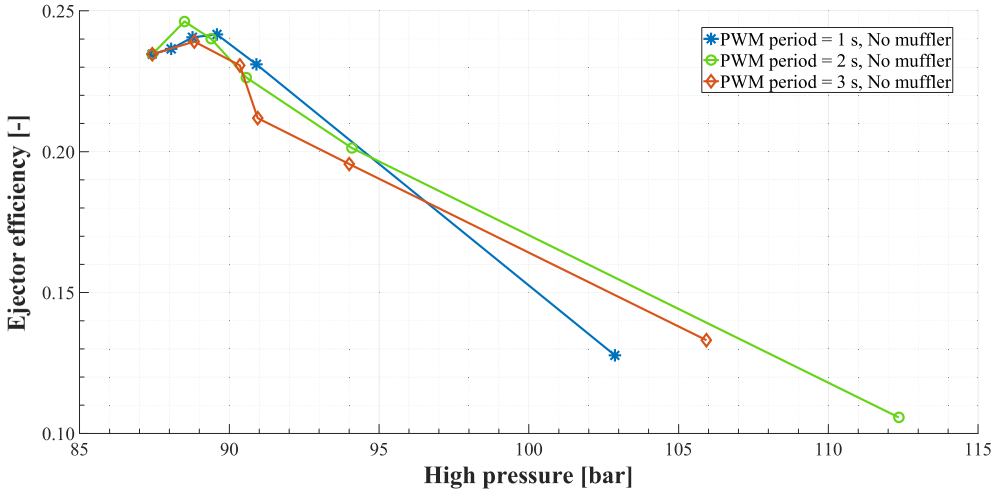

Fig. 4a. Ejector efficiency as a function of high pressure and PWM period (compressor speed = 50 Hz, $t_{water,gc\ in}$ = 35 °C, $t_{eg,evap\ in}$ = 5 °C, $\Delta T_{superheating}$ = 8 K).

found that the maximum discrepancy regarding the heat balance between R744 and the secondary fluids were within 3% in the evaporator and within 5% in the gas cooler.

3. Results and discussion

3.1. Proof of concept and influence of PWM period

The influence of the opening degree (OD) of the MSV on the motive nozzle pressure (from sensor indicated as P8 in Fig. 1), suction nozzle pressure (from sensor indicated as P9 in Fig. 1) and diffuser outlet pressure (from sensor indicated as P10 in Fig. 1) pressure is showed by using Figs. 2a–2e for the case based on PWM period = 2 s and no mufflers. The other pressures were not included (i) not to compromise the clarity of Fig. 2a–2e as well as (ii) they did not affect the conclusions drawn in this Subsection. It is important to highlight that the OD indicates the percentage of time during which MSV is open over the selected PWM period. For instance, OD = 90% refers to the case in which MSV is closed for 10% of the PWM period, whereas it is open for the remaining 90% of the PWM period. As shown in Fig. 2a, the PWM effect led to three consequences: (i) the occurrence of pressure oscillations on the high pressure side as the MSV opens and closes (fluid hammer effect), (ii) high pressure decrease and increase as the MSV opens and closes and (iii) increase of the suction pressure as the MSV closes resulting in the equalization with the diffuser (receiver) pressure. The lower the OD, the more evident the second and third consequences appear. A small decay of the diffuser outlet pressure occurs as the MSV closes and is thought to take place due to the frictional and accelerational pressure drop between the diffuser and the receiver. Likewise, the suction pressure and receiver pressure could equalize possibly through the expansion device, as the check valve on the ejector suction is thought to close completely at similar speeds as the MSV. However, despite the aforementioned pressure equalizations, Fig. 2a–2d reveal that a pressure lift above 4 bar is provided, while Fig. 2f shows that the refrigerant is still drawn from the intermediate pressure. This means that the advantage of having the ejector is largely prevailing with small inefficiency for bringing the suction pressure down during the opening. In addition, a pressure drop between the evaporator outlet and the ejector suction nozzle was found (Fig. 2f).

The influence of the high pressure and that of OD on COP at different PWM periods (i.e. 1 s, 2 s and 3 s) and no mufflers are depicted in Fig. 3a and 3b, respectively. It was brought to light that the high pressure can be risen from 87.4 bar (OD = 100%, i.e. passive ejector) to 102.9 bar (OD = 30%) at PWM period = 1 s, from 87.4 bar (OD = 100%, i.e. passive ejector) to 112.4 bar (OD = 30%) at PWM period = 2 s and from 87.4 bar (OD = 100%, i.e. passive ejector) to 105.9 bar (OD = 40%) at PWM

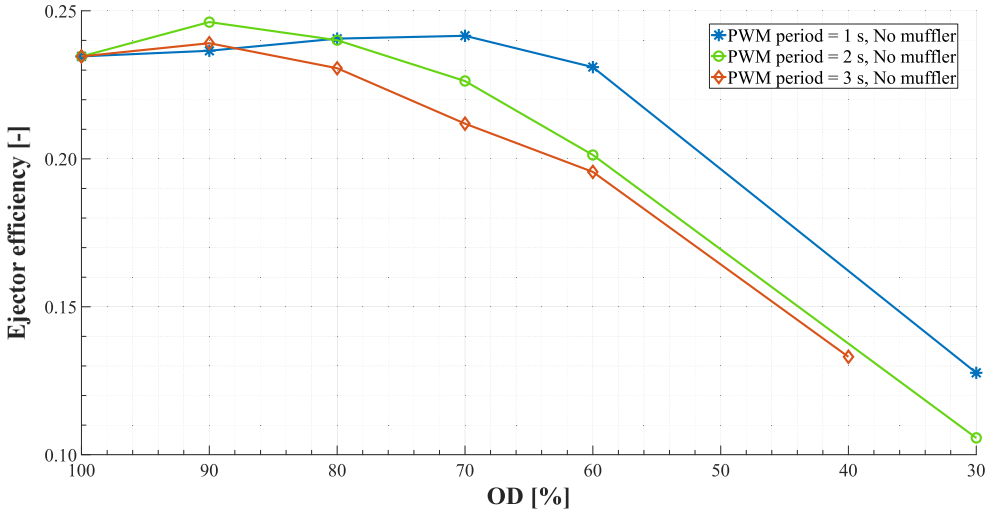

Fig. 4b. Ejector efficiency as a function of MSV opening degree (OD) and PWM period (compressor speed = 50 Hz, $t_{water,gc\ in}$ = 35 °C, $t_{eg,evap\ in}$ = 5 °C, $\Delta T_{superheating}$ = 8 K).

Table 4
Influence of PWM period on COP, cooling capacity and ejector efficiency at the optimal operating condition (compressor speed = 50 Hz, $t_{water,gc\ in}$ = 35 °C, $t_{eg,evap\ in}$ = 5 °C, $\Delta T_{superheating}$ = 8 K).

Scenario	COP [-]	$\dot{Q}_{eg,evap}$ [kW]	$\eta_{ejector}$ [-]
PWM ejector with PWM period = 1 s and no mufflers	1.672	2.187	0.241
PWM ejector with PWM period = 2 s and no mufflers	1.674	2.194	0.240
PWM ejector with PWM period = 3 s and no mufflers	1.672	2.203	0.231

period = 3 s. In case of PWM period = 2 s the highest gas cooler pressure was greater than that offered by both PWM period = 1 s and PWM period = 3 s. The former result was due to the need for OD < 30% to achieve high pressures above 112.4 bar. The latter outcome was a consequence of the presence of a safety device limiting the high pressure to 115 bar. Furthermore, the best COP values were achieved, i.e. about 1.67 at OD = 80% for all three evaluated PWM periods. The slight differences in COP revealed in Fig. 3a and 3b could be related to the enhancement in heat transfer within the heat exchangers as a consequence of the refrigerant pulsation. However, this needs to be shown by implementing an advanced simulation model (validated against experimental data) involving the dynamic behaviour of both the ejector and the system. It could be stated that the PWM ejector can control the gas cooler pressure, allowing a vapour-compression cooling unit to accomplish the best COP in transcritical operating conditions regardless of the selected PWM period. The difference in optimal value under the different selected PWM periods highlighted in Fig. 3a and 3b is believed to be a consequence of the transient thermodynamic state upstream of the motive nozzle as both pressure and temperature are unsteady as well as of the measurement equipment accuracy/calculated parameter experimental uncertainties.

The effect of high pressure and that of OD at the three selected PWM periods on the ejector efficiency, which was calculated by considering the pressure at the sensors mounted directly on the ejector housing, are presented in Fig. 4a and b, respectively. The results obtained suggest that at the optimum running modes the PWM ejector efficiencies could achieve the values of 0.241 for PWM period = 1 s, 0.240 for PWM period = 2 s and 0.239 for PWM period = 3 s, whereas it was equal to 0.235 for the passive ejector (OD = 100%). In Fig. 4a and b it is also highlighted

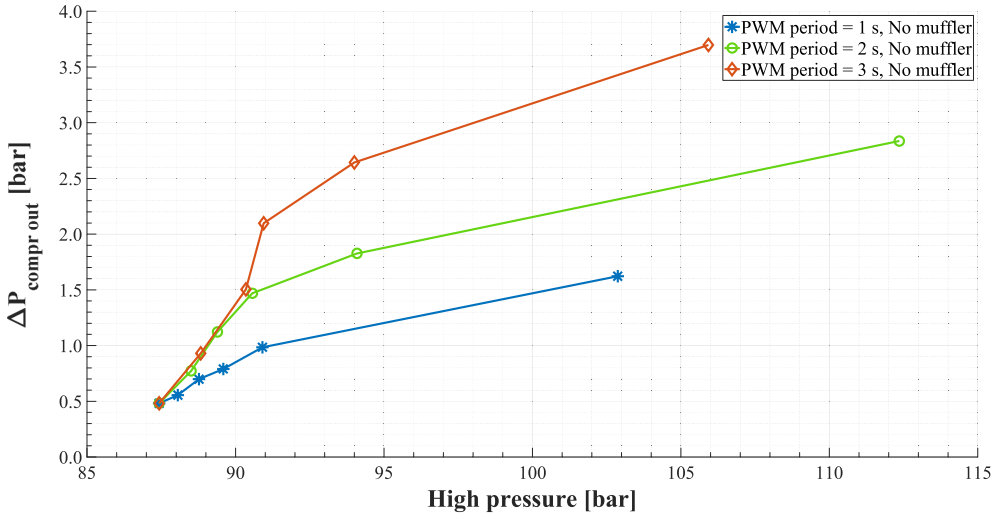

Fig. 5a. Maximum difference between the highest and the lowest value of pressure ($\Delta P_{compr\ out}$) over 10 s for the sensor between the compressor discharge and the mufflers as a function of high pressure and PWM period (compressor speed = 50 Hz, $t_{water,gc\ in}$ = 35 °C, $t_{eg,evap\ in}$ = 5 °C, $\Delta T_{superheating}$ = 8 K).

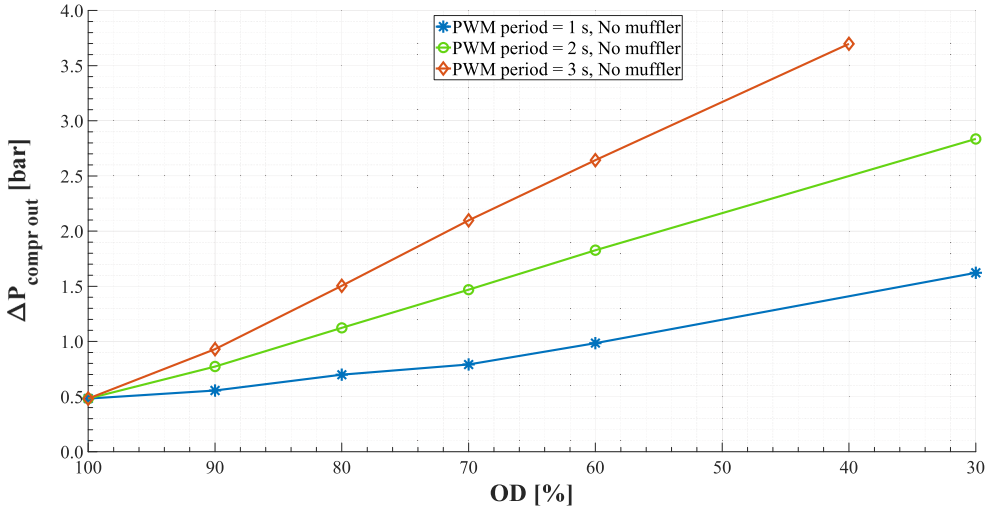

Fig. 5b. Maximum difference between the highest and the lowest value of pressure ($\Delta P_{compr\ out}$) over 10 s for the sensor between the compressor discharge and the mufflers as a function of opening degree (OD) of MSV and PWM period (compressor speed = 50 Hz, $t_{water,gc\ in}$ = 35 °C, $t_{eg,evap\ in}$ = 5 °C, $\Delta T_{superheating}$ = 8 K).

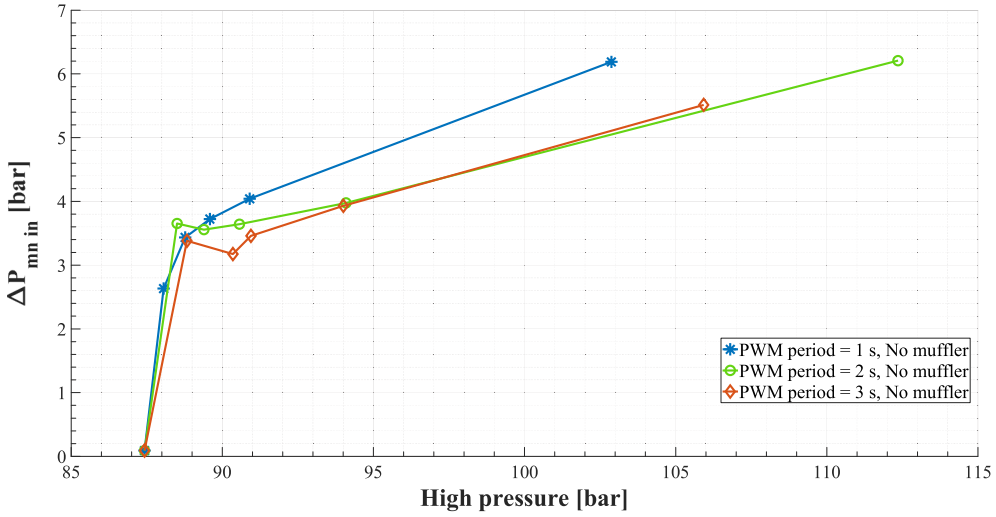

Fig. 6a. Maximum difference between the highest and the lowest value of pressure ($\Delta P_{mn\ in}$) over 10 s for the sensor upstream of the ejector motive nozzle as a function of high pressure and PWM period (compressor speed = 50 Hz, $t_{water,gc\ in}$ = 35 °C, $t_{eg,evap\ in}$ = 5 °C, $\Delta T_{superheating}$ = 8 K).

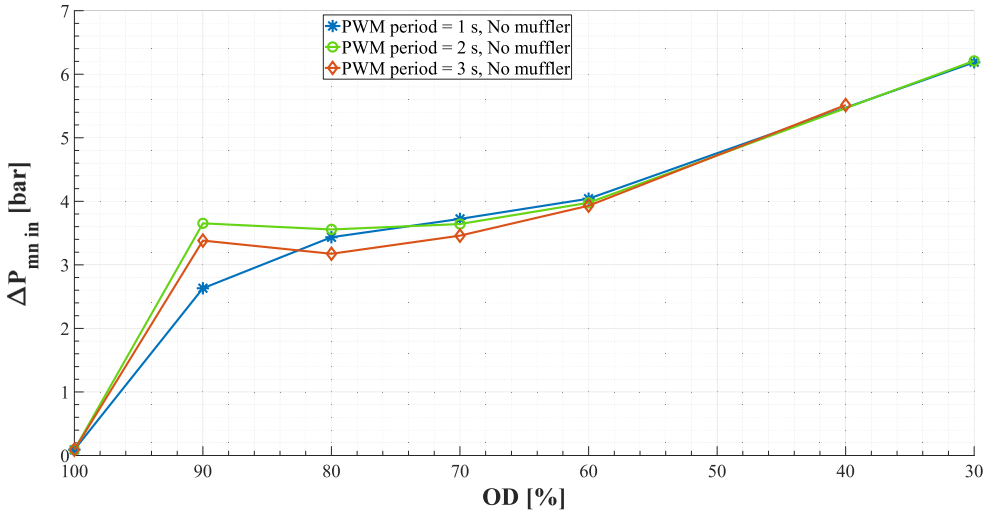

Fig. 6b. Maximum difference between the highest and the lowest value of pressure ($\Delta P_{mn\ in}$) over 10 s for the sensor upstream of the ejector motive nozzle as a function of MSV opening degree (OD) and PWM period (compressor speed = 50 Hz, $t_{water,gc\ in}$ = 35 °C, $t_{eg,evap\ in}$ = 5 °C, $\Delta T_{superheating}$ = 8 K).

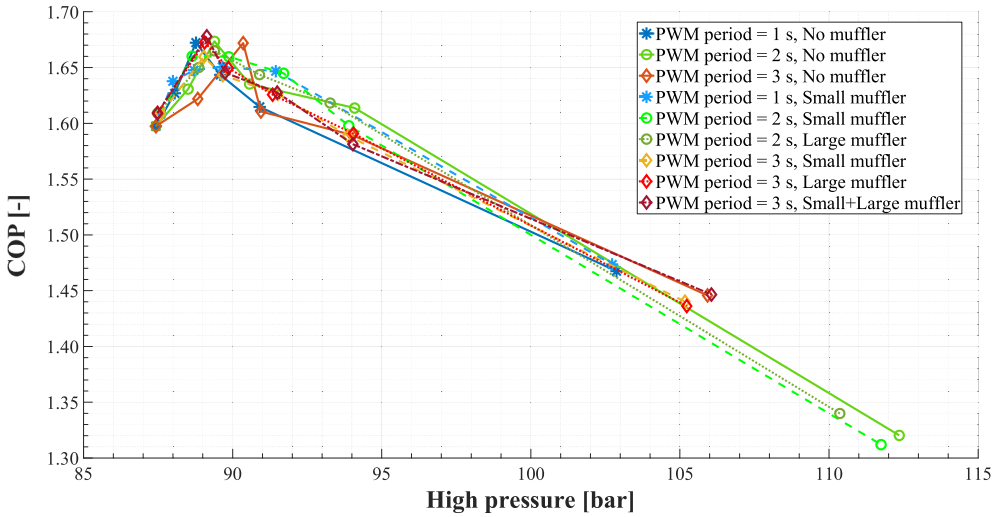

Fig. 7. COP at $t_{water,gc\ in}$ of 35 °C as a function of high pressure, PWM period and muffler size (compressor speed = 50 Hz, $t_{eg,evap\ in}$ = 5 °C, $\Delta T_{superheating}$ = 8 K).

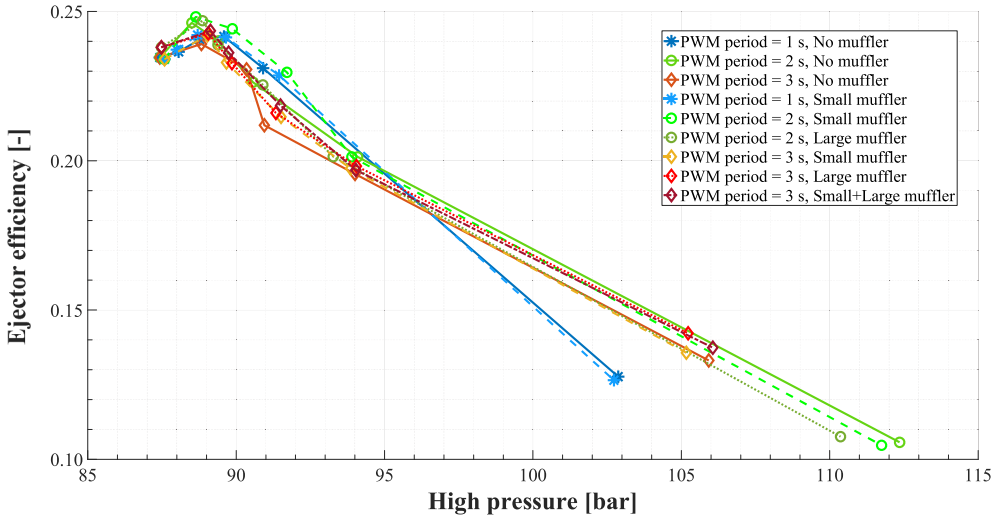

Fig. 8. Ejector efficiency at $t_{water,gc\ in}$ of 35 °C as a function of high pressure, PWM period and muffler size (compressor speed = 50 Hz, $t_{eg,evap\ in}$ = 5 °C, $\Delta T_{superheating}$ = 8 K).

Table 5
Influence of PWM period and muffler size on COP, cooling capacity and ejector efficiency at the optimal operating condition (compressor speed = 50 Hz, $t_{water,gc\ in}$ = 35 °C, $t_{eg,evap\ in}$ = 5 °C, $\Delta T_{superheating}$ = 8 K).

Scenario	COP [-]	$\dot{Q}_{eg,evap}$ [kW]	$\eta_{ejector}$ [-]
PWM ejector with PWM period = 1 s and small muffler	1.651	2.171	0.241
PWM ejector with PWM period = 2 s and small muffler	1.660	2.172	0.248
PWM ejector with PWM period = 2 s and large muffler	1.665	2.197	0.239
PWM ejector with PWM period = 3 s and small muffler	1.660	2.175	0.242
PWM ejector with PWM period = 3 s and large muffler	1.673	2.197	0.243
PWM ejector with PWM period = 3 s and small + large muffler	1.678	2.203	0.244

that the PWM ejector efficiencies are lower than those measured in a laboratory [10]. However, these values were actually underestimated, since they were averaged over the whole data collection period, i.e. including the period during which the diffuser outlet and the suction nozzle pressure equalized. In addition, the cooling capacity with respect to the high pressure and MSV opening degree at different PWM periods is presented in Appendix A.

The results summarized with the aid of Table 4 highlight that the most suitable PWM period could not be selected on the basis of the COP and PWM ejector efficiency alone. However, high pressure perturbations were found at low ODs, which are typically an unwanted instability. The maximum difference between the highest and the lowest value of pressure ($\Delta P_{compr\ out}$) over 10 s for the sensor installed between the compressor discharge and the mufflers (P1 in Fig. 1) and that ($\Delta P_{mn\ in}$) for the pressure sensor mounted upstream of the ejector motive nozzle (P8 in Fig. 1) are depicted in Figs. 5a and 5b, Figs. 6a and 6b. The figures show that the maximum pressure difference increase significantly with increasing PWM period and decreasing OD. Furthermore, larger pressure differences were found close to the MSV ($\Delta P_{mn\ in}$). The maximum pressure differences were above 5.5 bar for the investigated PWM periods at the lowest OD. Finally, the transient variation of R744 mass flow rates as a function of PWM period is described in Appendix B with the aid of the case involving OD = 60%.

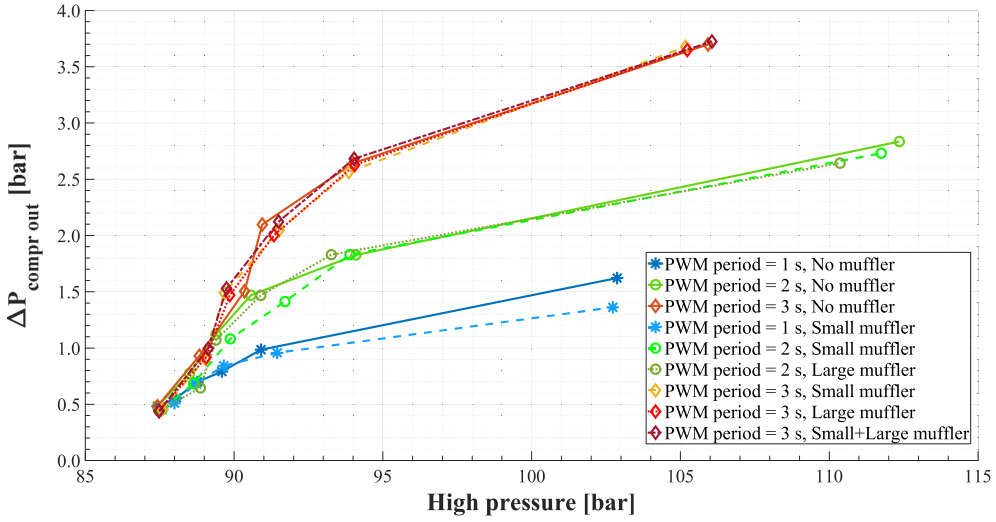

Fig. 9. Maximum difference between the highest and the lowest value of pressure ($\Delta P_{compr\ out}$) over 10 s for the sensor between the compressor discharge and the mufflers as a function of high pressure, PWM period and muffler size (compressor speed = 50 Hz, $t_{water,gc\ in}$ = 35 °C, $t_{eg,evap\ in}$ = 5 °C, $\Delta T_{superheating}$ = 8 K).

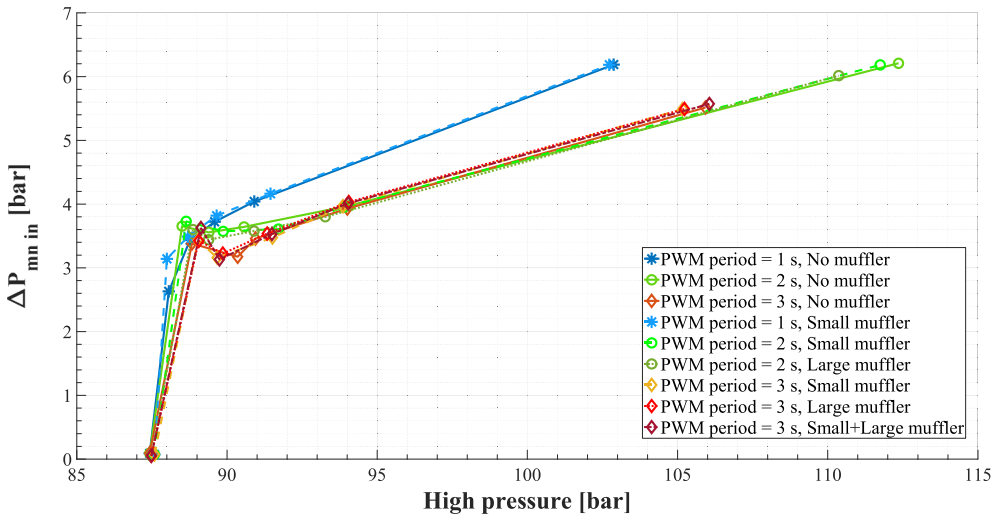

Fig. 10. Maximum difference between the highest and the lowest value of pressure ($\Delta P_{mn\ in}$) over 10 s for the sensor upstream of ejector motive nozzle (compressor speed = 50 Hz, $t_{water,gc\ in}$ = 35 °C, $t_{eg,evap\ in}$ = 5 °C, $\Delta T_{superheating}$ = 8 K).

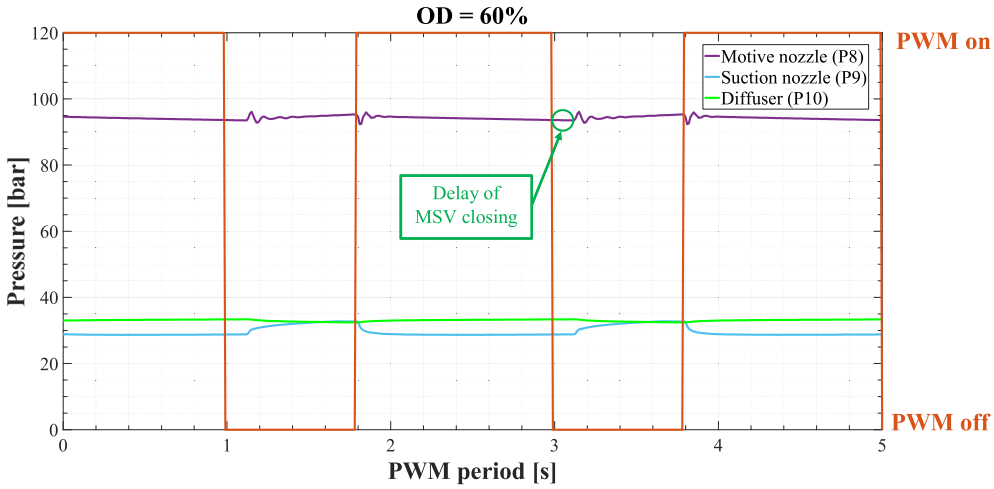

Fig. 11. Example of MSV closing delay visualization.

3.2. Influence of muffler volume

The influence of the muffler volume was investigated by the philosophy that larger buffers were necessary for higher PWM periods. Six additional experimental scenarios were measured at various ODs:

1. PWM period = 1 s and adoption of a small muffler (i.e. 0.8 L);
2. PWM period = 2 s and adoption of a small muffler (i.e. 0.8 L);
3. PWM period = 2 s and adoption of a large muffler (i.e. 1.6 L);
4. PWM period = 3 s and adoption of the small muffler (i.e. 0.8 L);
5. PWM period = 3 s and adoption of the large muffler (i.e. 1.6 L);
6. PWM period = 3 s and adoption of the small muffler and the large one simultaneously (i.e. 2.4 L).

The COP and the ejector efficiency for all the investigated cases are presented in Figs. 7 and 8, respectively. The results showed in Fig. 7 and Table 5 revealed that the COP values are not influenced by both the PWM period and the muffler volume considerably, being the difference in COP negligible for all the investigated cases. This means that the PWM ejector can appropriately control the gas cooler pressure, allowing a small-capacity unit to attain the best COP in transcritical regime regardless the selected PWM period and muffler volume. Similarly to the COP, Fig. 8 and Table 5 suggest that the ejector efficiency were not affected by the PWM period as well as the muffler volume substantially.

The results in terms of $\Delta P_{compr\ out}$ and $\Delta P_{mn\ in}$, which are respectively shown in Figs. 9 and 10, reveal the negligible influence of the muffler presence. It is worth remarking that in all the investigated cases, it was experienced that, regardless the PWM period, the adoption of muffler or not as well as the size of the possible adopted muffler:

- the PWM ejector can control the high pressure effectively;
- despite the pressure equalization mentioned above, the compressor draws the refrigerants from the intermediate pressure rather than from the low pressure.

An important consideration, which needs to be mentioned, is the delay in MSV closing as the PWM signal switched from ON to OFF. These results can be visualized with the aid of Fig. 11, in which the case involving OD = 60%, PWM = 2 s and no mufflers is reported. At the x-axis value in Fig. 11 of about 3 s, the PWM signal is OFF and thus MSV was supposed to be closed. However, Fig. 11 and Table 6 reveal that MSV had a delay in closing of about 0.13 s. This means that, on the one hand, MSV was supposed to be open for 60% (i.e. 1.20 s) of the PWM period (i.e. 2.00 s) and closed for the following 40% (i.e. 0.80 s) of the

Table 6
Delay (in seconds) in MSV closing as a function of PWM period and muffler size (compressor speed = 50 Hz, $t_{water,gc\ in}$ = 35 °C, $t_{eg,evap\ in}$ = 5 °C, $\Delta T_{superheating}$ = 8 K).

Scenario	OD = 90%	OD = 80%	OD = 70%	OD = 60%	OD = 40%	OD = 30%
PWM ejector with PWM period = 1 s and no mufflers	0.09	0.11	0.12	0.14	–	0.17
PWM ejector with PWM period = 1 s and small muffler	0.09	0.10	0.11	0.12	–	0.17
PWM ejector with PWM period = 2 s and no mufflers	0.08	0.10	0.11	0.14	–	0.18
PWM ejector with PWM period = 2 s and small muffler	0.08	0.09	0.10	0.13	–	0.18
PWM ejector with PWM period = 2 s and large muffler	0.07	0.10	0.11	0.14	–	0.20
PWM ejector with PWM period = 3 s and no mufflers	0.07	0.09	0.11	0.12	0.16	–
PWM ejector with PWM period = 3 s and small muffler	0.07	0.08	0.11	0.12	0.17	–
PWM ejector with PWM period = 3 s and large muffler	0.07	0.10	0.11	0.13	0.17	–
PWM ejector with PWM period = 3 s and small + large muffler	0.07	0.10	0.11	0.13	0.17	–

PWM period (i.e. 2.00 s). On the other hand, it was actually experienced that MSV was open for about 66.5% (i.e. about 1.33 s) of the PWM period (i.e. 2.00 s) and closed for about the following 33.5% (i.e. about 0.67 s) of the PWM period (i.e. 2.00 s). This can explain the reason why the high pressure did not vary significantly at high OD of MSV (see for example Fig. 3a) for which even a small delay in MSV closing could significantly affect the control of this parameter. It is also possible to notice in Table 6 that the delay mentioned above increased with decrease in OD. This was found to be more depending on the OD rather than on the PWM period, leading the case relying on PWM period = 1 s to be more influenced by the delay in MSV closing. As an example, considering the scenarios involving OD = 90% and no mufflers, the actual OD was 99.0% for PWM period = 1 s, 94.0% for PWM period = 2 s and 92.3% for PWM period = 3 s. As for the case relying on PWM period = 3 s, this was found to offer similar values of COP and ejector efficiency to the cases based on PWM period = 2 s. However, the latter was characterized by lower pressure fluctuations on the high pressure side, offering higher ejector and system lifetime. Therefore, taking into account that no mufflers are usually mounted in small-capacity solutions, it can be claimed that the PWM ejector in the employed test rig should operate with a PWM period of 2 s and without mufflers. As additional remarks, it is thought that in large-capacity applications the use of mufflers could also be avoided as a consequence of the adoption of larger heat exchangers (e.g. display cabinets and air-cooled gas coolers), which should dampen the fluctuations resulting from the PWM effect. As regards the PWM period, the authors think that at this stage it is difficult to generalize the results regarding an optimal PWM period, as it is needed to implement a control system tailored to the PWM ejector with respect to the operating conditions (e.g. eliminating the delay in MSV closing).

In addition, initial verification of the concept was performed without considering the effect of both the PWM period and the muffler volume [14,15]. Nevertheless, in the present work the PWM period and the use of mufflers were not considered at heat sink temperatures above 35 °C, since these running modes occur much less frequently in condensing units operating in the European climate context. Also, the selection of the PWM period of 2 s and no mufflers would have been suitable for heat sink temperatures below 35 °C too, as at these running modes the phenomena described in Subsection 3.1 would have been less noticeable [15]. This means that the PWM period would have been chosen on the same basis as in the present work as well as the use of mufflers would have been unnecessary. Such a conclusion can be extended to the cases involving higher evaporation temperatures, as showed by Gullo [14]. However, the results presented by Gullo et al. [15] and Gullo [14] were obtained using a less instrumented and well-defined test system, whose quality and accuracy needed to be enhanced. The results described in the present work were collected after recalibrating/replacing the experimental equipment meticulously.

3.3. PWM ejector vs. Passive ejector vs. Standard mode

In this Subsection the performance of the standard solution (i.e. with flash gas by-pass valve and without ejector), the system with passive ejector (i.e. without flow modulation) and the unit with PWM ejector are compared at compressor speed = 50 Hz, $t_{water,gc\ in}$ = 35 °C, $t_{eg,evap\ in}$ = 5 °C and $\Delta T_{superheating}$ = 8 K. The high pressure of the standard solution was varied between about 80 bar and 98 bar in order to evaluate the maximum COP value, which was found to be about equal to 1.51 (obtained at roughly P_{gc} = 90.9 bar), leading to a cooling capacity of about 1.94 kW. Also, its intermediate pressure was set to 35 bar. As for the system with passive ejector, at the aforementioned running modes COP, cooling capacity and ejector efficiency were 1.60, 2.07 kW and 0.235, respectively. In accordance with Tables 4 and 5, the unit with PWM ejector was capable of enhancing COP and cooling capacity respectively by up to about 10.8% and 13.4% compared to the standard solution. As the unit with PWM ejector was benchmarked to the system with passive ejector, it was found that the new solution offered improvements of cooling capacity, COP and ejector efficiency above 6%, 5% and 6%, respectively. It is worth remarking that its today's available competitors, i.e. needle-based ejector and vortex-based ejector, present COP enhancements by 2%–4% in comparison with the passive ejector [35,65]. In particular, the PWM ejector involving the PWM period = 2 s and no mufflers featured enhancements in COP by 9.7% compared to the standard solution and by 3.9% over the system with passive ejector.

4. Conclusions and future developments

Small-capacity transcritical R744 vapour-compression systems (e.g. condensing units) outfitted with two-phase ejectors are thought to be key elements for a zero-carbon future. However, at present condensing units cannot benefit from the energy advantageous offered by two-phase ejectors, since the flow modulation of these expansion work recovery devices cannot be effectively implemented in small-capacity applications. Therefore, in order to bridge this knowledge gap an innovative flow modulation mechanism has been proposed and investigated. The new technique is based on the pulse-width modulation (PWM) of R744 flow through the ejector. The proposed methodology features low cost, simplicity and low vulnerability to clogging. The study has involved the assessment of the advantageous deriving from the presence of mufflers

having different size (0.8 L, 1.6 L, 2.4 L) as well as from various PWM periods (1 s, 2 s, 3 s).

At the compressor speed of 50 Hz, water temperature at the gas cooler inlet of 35 °C and R744 evaporating temperature of about −5 °C, the gathered experimental data show that the high pressure can be controlled properly as well as augmented from about 87 bar to 112 bar, proving the effectiveness of the proposed mechanism. In addition, the results obtained have suggested that the performance of both the PWM ejector and the system is not affected by the PWM period as well as the installation of mufflers is not required. Therefore, the results obtained suggest the adoption of a PWM period of 2 s, being the case involving PWM period of 1 s affected by a delay in motive solenoid valve closing more significantly and that relying on PWM period of 3 s characterized by higher pressure fluctuations. It is important to highlight that the use of mufflers could be avoided in large-capacity applications as well, whereas at this stage it is challenging to generalize the outcomes associated with the optimum PWM period. Compared to standard solution (i.e. with flash gas by-pass valve and without ejector), the solution with PWM ejector can enhance COP and cooling capacity by up to about 10.8% (by 9.7% with PWM period = 2 s and no mufflers) and 13.4%. As the system with passive ejector (i.e. without flow modulation) is selected as the baseline, the proposed solution can improve COP and cooling capacity by above 5% (by 3.9% with PWM period = 2 s and no mufflers) and 6%. It is worth observing that its today's available competitors, i.e. needle-based ejector and vortex-based ejector, offer COP improvements by 2%–4% compared to the passive ejector. Also, the investigated solution can be further enhanced by implementing a detailed simulation model (validated against experimental data) describing the dynamic behaviour of both the ejector and the system. Further benefits could be obtained by implementing a control system tailored to the PWM ejector with respect to the operating conditions so as to maximize the COP all year round. Finally, although the PWM working principle has been thought for small-capacity vapour-compression systems, it has no practical size or application constraints.

As future work, it is needed to:

- study the effect of the compressor speed and water temperature at the gas cooler inlet on the performance of both the PWM ejector and the overall system;
- investigate the potential energy benefits of the PWM ejector in air conditioning units;
- quantify the energy advantageous deriving from the adoption of overfed evaporators;
- investigate the potential energy benefits of the PWM ejector in subcritical and transition regime.

CRediT authorship contribution statement

Paride Gullo: Conceptualization, Methodology, Investigation, Writing - original draft, Funding acquisition. **Michael Birkelund:** Conceptualization, Writing - review & editing, Supervision. **Ekaterini E. Kriezi:** Writing - review & editing, Supervision. **Martin Ryhl Kærn:** Conceptualization, Methodology, Resources, Writing - review & editing.

Declaration of Competing Interest

The authors declare that they have no known competing financial interests or personal relationships that could have appeared to influence the work reported in this paper.

Acknowledgements

The research leading to these results has received funding from the European Union's Horizon 2020 research and innovation programme under the Marie Skłodowska-Curie grant agreement No. 844924 (Project: ECO_2-RAPJECT).

Appendix A

The effect of the high pressure and that of the MSV opening degree (OD) on the cooling capacity (see numerator of Eq. (1)) at different PWM periods (i.e. 1 s, 2 s and 3 s) are presented in Figs. A.1 and A.2, respectively. In the selected example, no mufflers were taken into account.

It was observed that the cooling capacity can be increased from 2.07 kW at 87.42 bar (OD = 100%, i.e. passive ejector) to 2.19 kW at 88.77 bar (OD = 80%) for PWM period = 1 s, from 2.07 kW at 87.42 bar (OD = 100%, i.e. passive ejector) to 2.19 kW at 89.39 bar (OD = 80%) for PWM period = 2 s and from 2.07 kW at 87.43 bar (OD = 100%, i.e. passive ejector) to 2.20 kW at 90.35 bar (OD = 80%) for PWM period = 3 s. A decreasing trend was assessed at OD ≥ 70%, leading to a cooling capacity of 2.06 kW at OD = 30% for PWM period = 1 s, of 1.94 kW at OD = 30% for PWM period = 2 s and of 2.05 kW at OD = 40% for PWM period = 3 s. The experienced behaviour is consistent with the experimental measurements collected by Elbel and Hrnjak [8].

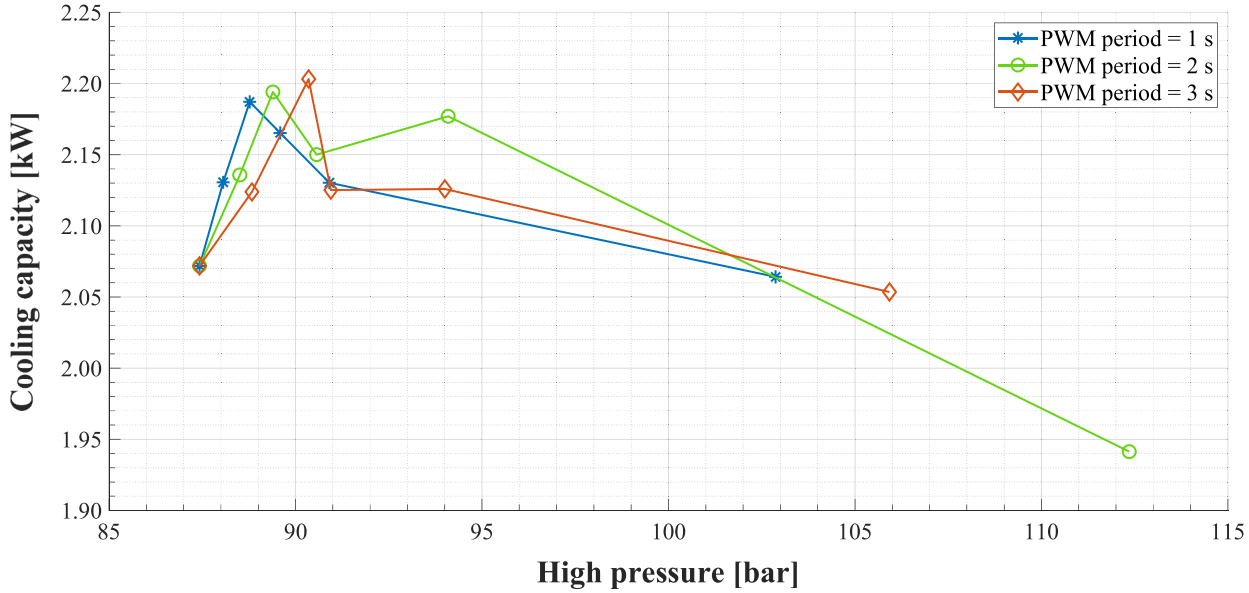

Fig. A1. Cooling capacity as a function of high pressure and PWM period (compressor speed = 50 Hz, $t_{water,gc\ in}$ = 35 °C, $t_{eg,evap\ in}$ = 5 °C, $\Delta T_{superheating}$ = 8 K).

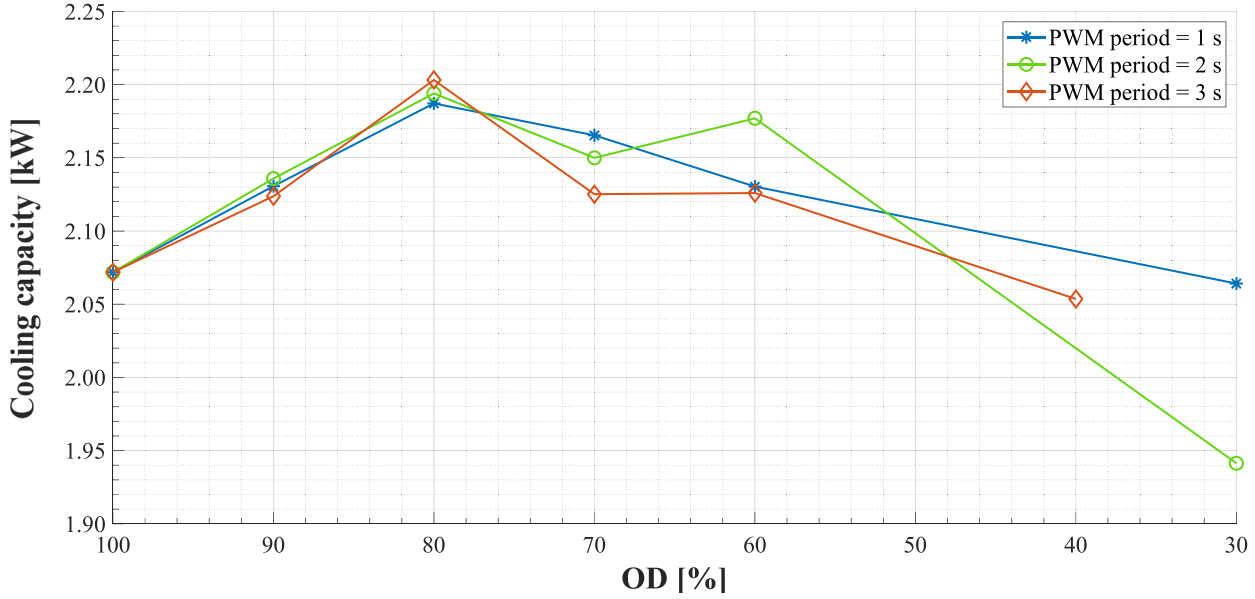

Fig. A2. Cooling capacity as a function of MSV opening degree (OD) and PWM period (compressor speed = 50 Hz, $t_{water,gc\ in}$ = 35 °C, $t_{eg,evap\ in}$ = 5 °C, $\Delta T_{superheating}$ = 8 K).

Appendix B

The transient variation of R744 mass flow rates at PWM period of 1 s, 2 s and 3 s for the case involving the MSV opening degree (OD) of 60% is presented in Figs. B.1, B.2 and B.3, respectively. As showed in Fig. B.1, both the R744 mass flow rate measured by the mass flow meter at the high pressure side (see Fig. 1) and the R744 mass flow rate measured by the mass flow meter at the intermediate pressure side (see Fig. 1) are not affected significantly by the pulsation of the refrigerant flow through the ejector. However, for the case involving PWM period = 2 s (see Fig. B.2) the R744 mass flow rate measured by the mass flow meter at the intermediate pressure side was found to behave similarly to the suction pressure (see Fig. 2d) as the motive solenoid valve closes. This is thought to be a consequence of the increase in suction pressure resulting from the motive solenoid valve closing. Finally, the case based on PWM period = 3 s revealed that the transient variation of both R744 mass flow rates are influenced considerably by the pulsation of the refrigerant flow through the ejector. This is believed to be the result of the substantial pressure fluctuations on the high pressure side (see Fig. 5a and b) as well as of the increment in suction pressure as the motive solenoid valve closes (see Fig. 2d).

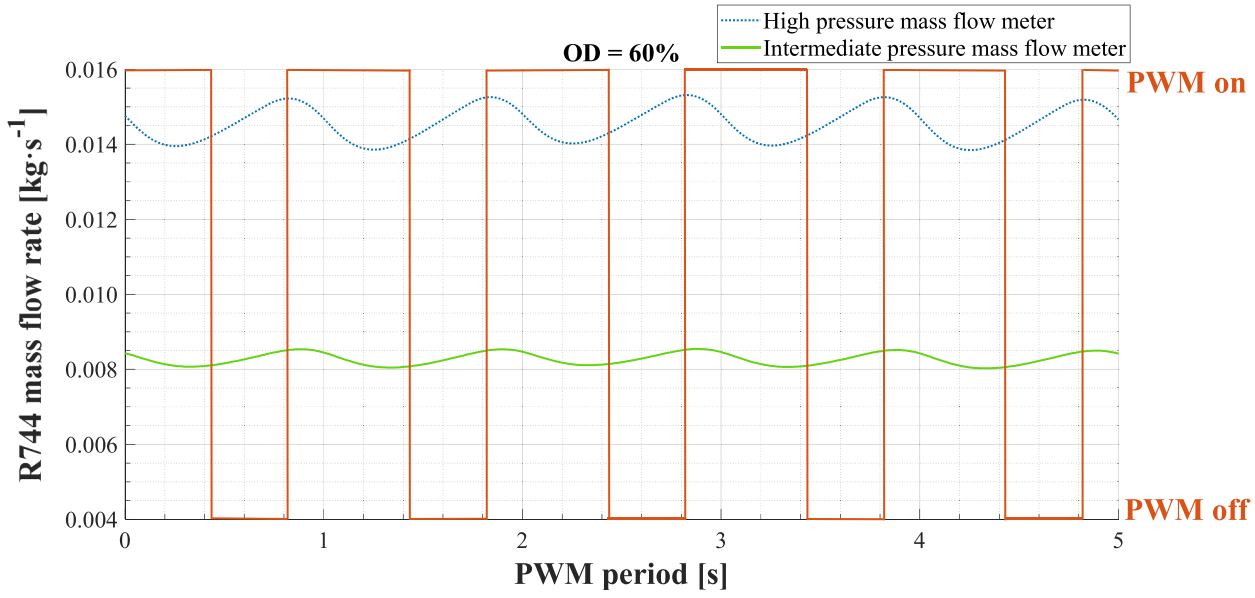

Fig. B1. Transient variation of R744 mass flow rates at PWM period of 1 s, MSV opening degree (OD) of 60% and without mufflers (compressor speed = 50 Hz, $t_{water,gc\ in}$ = 35 °C, $t_{eg,evap\ in}$ = 5 °C, $\Delta T_{superheating}$ = 8 K).

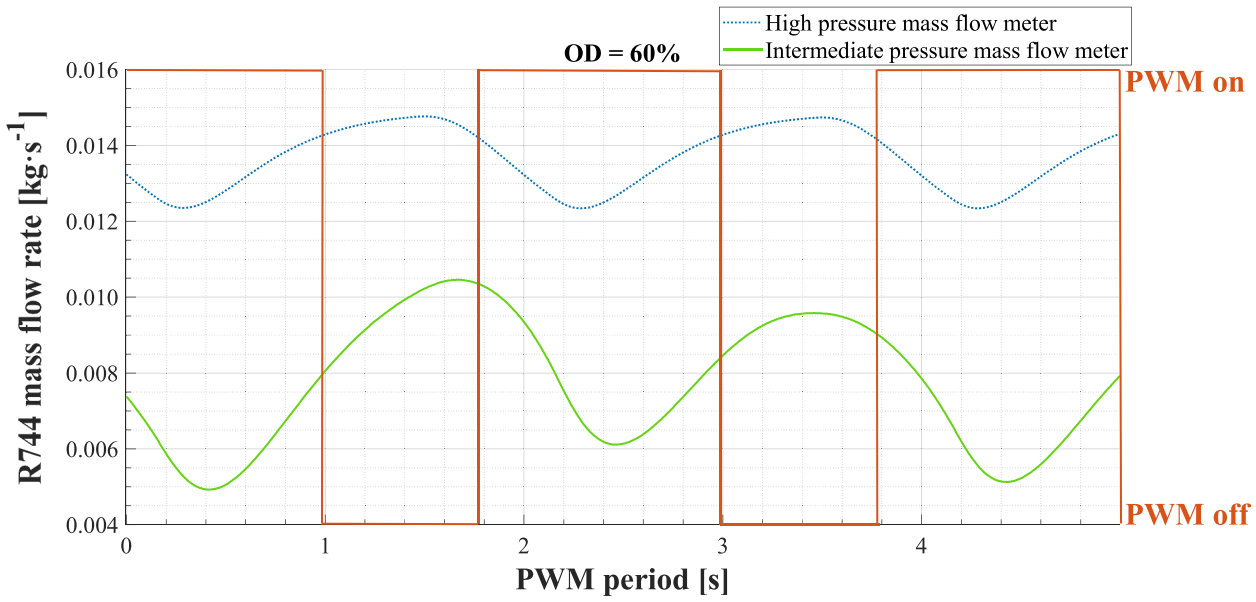

Fig. B2. Transient variation of R744 mass flow rates at PWM period of 2 s, MSV opening degree (OD) of 60% and without mufflers (compressor speed = 50 Hz, $t_{water,\ gc\ in}$ = 35 °C, $t_{eg,evap\ in}$ = 5 °C, $\Delta T_{superheating}$ = 8 K).

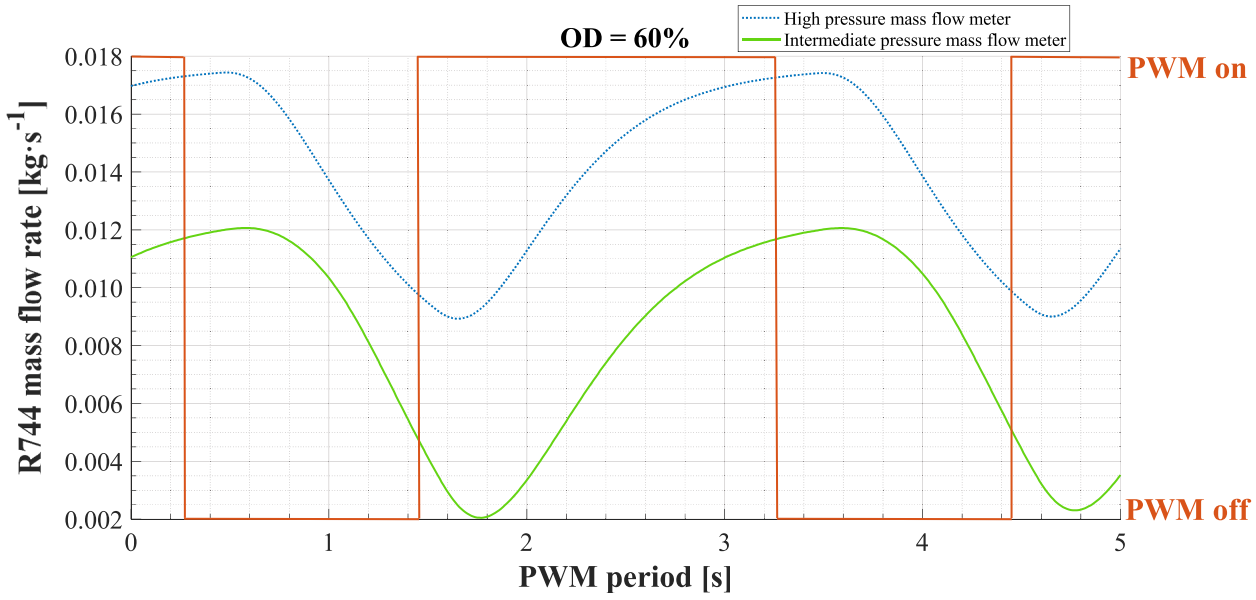

Fig. B3. Transient variation of R744 mass flow rates at PWM period of 3 s, MSV opening degree (OD) of 60% and without mufflers (compressor speed = 50 Hz, $t_{water,\ gc\ in}$ = 35 °C, $t_{eg,evap\ in}$ = 5 °C, $\Delta T_{superheating}$ = 8 K).

References

[1] Banasiak K, Hafner A, Kriezi EE, Madsen KB, Birkelund M, Fredslund K, et al. Development and performance mapping of a multi-ejector expansion work recovery pack for R744 vapour compression units. Int J Refrig 2015;57:265–76. https://doi.org/10.1016/j.ijrefrig.2015.05.016.

[2] Boccardi G, Botticella F, Lillo G, Mastrullo R, Mauro AW, Trinchieri R. Experimental investigation on the performance of a transcritical CO_2 heat pump with multi-ejector expansion system. Int J Refrig 2017;82:389–400. https://doi.org/10.1016/j.ijrefrig.2017.06.013.

[3] Bodys J, Palacz M, Haida M, Smolka J, Nowak AJ, Banasiak K, et al. Full-scale multi-ejector module for a carbon dioxide supermarket refrigeration system: Numerical study of performance evaluation. Energy Convers Manage 2017;138:312–26. https://doi.org/10.1016/j.enconman.2017.02.007.

[4] Bodys J, Smolka J, Palacz M, Haida M, Banasiak K, Nowak AJ, et al. Performance of fixed geometry ejectors with a swirl motion installed in a multi-ejector module of a CO_2 refrigeration system. Energy 2016;117:620–31. https://doi.org/10.1016/j.energy.2016.07.037.

[5] Cavallini A, Zilio C. Carbon dioxide as a natural refrigerant. Int J Low-Carbon Technol 2007;2(3):225–49. https://doi.org/10.1093/ijlct/2.3.225.

[6] Dai B, Zhao X, Liu S, Yang Q, Zhong D, Hao Y, et al. Energetic, exergetic and exergoeconomic assessment of transcritical CO_2 reversible system combined with dedicated mechanical subcooling (DMS) for residential heating and cooling. Energy Convers Manage 2020;209:112594. https://doi.org/10.1016/j.enconman.2020.112594.

[7] Elbel S, Lawrence N. Review of recent developments in advanced ejector technology. Int J Refrig 2016;62:1–18. https://doi.org/10.1016/j.ijrefrig.2015.10.031.

[8] Elbel S, Hrnjak P. Experimental validation of a prototype ejector design to reduce throttling losses encountered in transcritical R744 system operate. Int J Refrig 2008;31:411–22. https://doi.org/10.1016/j.ijrefrig.2007.07.013.

[9] F-Chart Software, 2020. Engineering Equation Solver (EES), Academic Professional V10.836-3D. Available at: <http://www.fchartsoftware.com/ees/> [accessed 08.01.2021].

[10] Fredslund K, Kriezi EE, Madsen KB, Birkelund M, Olsson R. CO_2 installations with a multi ejector for supermarkets, case studies from various locations. August; Edinburgh, UK. ID: 1105; 2016.

[11] Ge YT, Tassou SA. Control optimizations for heat recovery from CO_2 refrigeration systems in supermarket. Energy Convers Manage 2014;78:245–52. https://doi.org/10.1016/j.enconman.2013.10.071.

[12] Girotto, S., 2017. Improved transcritical CO2 refrigeration systems for warm climates. In: Proceedings of the 7th IIR Ammonia and CO2 Refrigeration Technologies Conference, 11th - 13th May; Ohrid, Macedonia.

[13] Gullo, P., 2021. Impact and quantification of various individual thermodynamic improvements for transcritical R744 supermarket refrigeration systems based on advanced exergy analysis. Energy Conversion and Management 229, 113684. DOI: 10.1016/j.enconman.2020.113684.

[14] Gullo, P., 2020. A novel capacity control mechanism for two-phase ejectors in transcritical R744 air conditioners. In: Proceedings of the ATMO/DTI Technical Conference on the Future of Air Conditioning, 23rd – 24th June; Online conference.

[15] Gullo P, Kærn MR, Birkelund M, Kriezi EE. Preliminary experimental investigation on a transcritical R744 condensing unit using the novel PWM ejector. In Proceedings of the 14th IIR-Gustav Lorentzen Conference on Natural Refrigerants. 2020.

[16] Gullo P, Kærn MR, Haida M, Smolka J, Elbel S. A review on current status of capacity control techniques for two-phase ejectors. Int J Refrig 2020;119:64–79. https://doi.org/10.1016/j.ijrefrig.2020.07.014.

[17] Gullo P. Innovative fully integrated transcritical R744 refrigeration systems for HFC-free future of supermarkets in warm and hot climates. Int J Refrig 2019;108:283–310. https://doi.org/10.1016/j.ijrefrig.2019.09.001.

[18] Gullo P, Hafner A, Banasiak K, Minetto S, Kriezi EE. Multi-ejector concept: a comprehensive review on its latest technological developments. Energies 2019;12(3):406. https://doi.org/10.3390/en12030406.

[19] Gullo P, Hafner A, Banasiak K. Transcritical R744 refrigeration systems for supermarket applications: Current status and future perspectives. Int J Refrig 2018;93:269–310. https://doi.org/10.1016/j.ijrefrig.2018.07.001.

[20] Gullo P, Tsamos KM, Hafner A, Banasiak K, Ge YT, Tassou SA. Crossing CO_2 equator with the aid of multi-ejector concept: a comprehensive energy and environmental comparative study. Energy 2018;164:236–63. https://doi.org/10.1016/j.energy.2018.08.205.

[21] Gullo P, Hafner A, Cortella G. Multi-ejector R744 booster refrigerating plant and air conditioning system integration – A theoretical evaluation of energy benefits for supermarket applications. Int J Refrig 2017;75:164–76. https://doi.org/10.1016/j.ijrefrig.2016.12.009.

[22] Gullo P, Cortella G, Minetto S, Polzot A. Overfed evaporators and parallel compression in commercial R744 booster refrigeration systems – An assessment of energy benefits. August; Edinburgh, UK. ID: 1039; 2016.

[23] Gullo P, Elmegaard B, Cortella G. Advanced exergy analysis of a R744 booster refrigeration system with parallel compression. Energy 2016;107:562–71. https://doi.org/10.1016/j.energy.2016.04.043.

[24] Gullo P, Elmegaard B, Cortella G. Energy and environmental performance assessment of R744 booster supermarket refrigeration systems operating in warm climates. Int J Refrig 2016;64:61–79. https://doi.org/10.1016/j.ijrefrig.2015.12.016.

[25] Hafner, A., Banasiak, K., Fredslund, K., Girotto, S., Smolka, J., 2016. R744 ejector system case: Italian supermarket, Spiazzo. In: Proceedings of the 12th IIR Gustav Lorentzen Natural Working Fluids Conference, 21st – 24th August; Edinburgh, UK. ID: 1078.

[26] Hafner A, Försterling S, Banasiak K. Multi-ejector concept for R-744 supermarket refrigeration. Int J Refrig 2014;43:1–13. https://doi.org/10.1016/j.ijrefrig.2013.10.015.

[27] Haida M, Palacz M, Bodys J, Smolka J, Gullo P, Nowak AJ. An experimental investigation of performance and instabilities of the R744 vapour compression rack equipped with a two-phase ejector based on short-term, long-term and unsteady operations. Appl Therm Eng 2021;185:116353. https://doi.org/10.1016/j.applthermaleng.2020.116353.

[28] Haida M, Smolka J, Hafner A, Palacz M, Ostrowski Z, Bodys J, et al. Performance operation of liquid ejectors for a R744 integrated multi-ejector supermarket system using a hybrid ROM. Int J Refrig 2020;110:58–74. https://doi.org/10.1016/j.ijrefrig.2019.10.020.

[29] Haida M, Smolka J, Hafner A, Ostrowski Z, Palacz M, Madsen KB, et al. Performance mapping of the R744 ejectors for refrigeration and air conditioning supermarket application: A hybrid reduced-order model. Energy 2018;153:933–48. https://doi.org/10.1016/j.energy.2018.04.088.

[30] Haida M, Banasiak K, Smolka J, Hafner A, Eikevik TM. Experimental analysis of the R744 vapour compression rack equipped with the multi-ejector expansion work recovery module. Int J Refrig 2016;64:93–107. https://doi.org/10.1016/j.ijrefrig.2016.01.017.

[31] He Y, Deng J, Li Y, Ma M. A numerical contrast on the adjustable and fixed transcritical CO_2 ejector using exergy flux distribution analysis. Energy Convers Manage 2019;196:729–38. https://doi.org/10.1016/j.enconman.2019.06.031.

[32] Kærn MR, Song Y, Markussen WB, Elmegaard B. Comparison of a CO_2 refrigeration and heat pump test system with and without ejector. Valencia, Spain. ID: 1290; 2018.

[33] Karampour M, Mateu-Royo C, Rogstam J, Sawalha S. Geothermal storage integration into a supermarket's CO_2 refrigeration system. Int J Refrig 2019;106:492–505. https://doi.org/10.1016/j.ijrefrig.2019.05.026.

[34] Kim M-H, Pettersen J, Bullard CW. Fundamental process and system design issues in CO_2 vapor compression systems. Prog Energy Combust Sci 2004;30(2):119–74. https://doi.org/10.1016/j.pecs.2003.09.002.

[35] Lawrence N, Elbel S. Experimental investigation on control methods and strategies for off-design operation of the transcritical R744 two-phase ejector cycle. Int J Refrig 2019;106:570–82. https://doi.org/10.1016/j.ijrefrig.2019.04.020.

[36] Lemmon, E.W., Bell, I.H., Huber, M.L., McLinden, M.O., 2018. NIST Standard Reference Database 23: Reference Fluid Thermodynamic and Transport Properties-REFPROP, Version 10.0, National Institute of Standards and Technology, Standard Reference Data Program.

[37] Liu F, Groll EA, Ren J. Comprehensive experimental performance analyses of an ejector expansion transcritical CO_2 system. Appl Therm Eng 2016;98:1061–9. https://doi.org/10.1016/j.applthermaleng.2015.12.017.

[38] Liu F, Groll EA, Li D. Modeling study of an ejector expansion residential CO_2 air conditioning system. Energy Build 2012;53:127–36. https://doi.org/10.1016/j.enbuild.2012.07.008.

[39] Liu F, Groll EA, Li D. Investigation on performance of variable geometry ejectors for CO_2 refrigeration cycles. Energy 2012;45(1):829–39. https://doi.org/10.1016/j.energy.2012.07.008.

[40] Liu F, Li Y, Groll EA. Performance enhancement of CO_2 air conditioner with a controllable ejector. Int J Refrig 2012;35(6):1604–16. https://doi.org/10.1016/j.ijrefrig.2012.05.005.

[41] Liu F, Groll EA. Study of ejector efficiencies in refrigeration cycles. Appl Therm Eng 2013;52(2):360–70. https://doi.org/10.1016/j.applthermaleng.2012.12.001.

[42] Liu, F., Groll, E.A., 2008. Analysis of a Two Phase Flow Ejector For Transcritical CO2 Cycle. In: Proceedings of the 12th International Refrigeration and Air Conditioning Conference at Purdue, 14th – 17th July; West Lafayette, USA. ID: 924.

[43] Lorentzen, G., 1994. Revival of carbon dioxide as a refrigerant. International Journal of Refrigeration 17(5), 292-301. DOI: 10.1016/j.ijrefrig.2017.06.013.

[44] Luger C, Rieberer R. Multi-objective design optimization of a rail HVAC CO_2 cycle. Int J Refrig 2018;92:133–42. https://doi.org/10.1016/j.ijrefrig.2018.05.033.

[45] Madsen KB, Kriezi EK. Financial aspects of ejector solutions in supermarket and smaller industrial systems. Valencia, Spain. ID: 1403; 2018.

[46] Mastrullo R, Mauro AW, Perrone A. A model and simulations to investigate the effects of compressor and fans speeds on the performance of CO_2 light commercial refrigerators. Appl Therm Eng 2015;84:158–69. https://doi.org/10.1016/j.applthermaleng.2015.03.035.

[47] Nakagawa M, Marasigan AR, Matsukawa T. Experimental investigation on the effect of internal heat exchanger in transcritical CO_2 refrigeration cycle with ejector. Int J Refrig 2011;34(7):1577–86. https://doi.org/10.1016/j.ijrefrig.2010.03.007.

[48] Palacz M, Smolka J, Kus W, Fic A, Bulinski Z, Nowak AJ, et al. CFD-based shape optimisation of a CO_2 two-phase ejector mixing section. Appl Therm Eng 2016;95:62–9. https://doi.org/10.1016/j.applthermaleng.2015.11.012.

[49] Polzot A, Gullo P, D'Agaro P, Cortella G. Performance evaluation of a R744 booster system for supermarket refrigeration, heating and DHW. August; Edinburgh, UK. ID: 1022; 2016.

[50] Polzot A, D'Agaro P, Gullo P, Cortella G. Modelling commercial refrigeration systems coupled with water storage to improve energy efficiency and perform heat recovery. Int J Refrig 2016;69:313–23. https://doi.org/10.1016/j.ijrefrig.2016.06.012.

[51] Purohit N, Gupta DK, Dasgupta MS. Experimental investigation of a CO_2 trans-critical cycle with IHX for chiller application and its energetic and exergetic evaluation in warm climate. Appl Therm Eng 2018;136:617–32. https://doi.org/10.1016/j.applthermaleng.2018.03.044.

[52] Purohit N, Gullo P, Dasgupta MS. Comparative assessment of low-GWP based refrigerating plants operating in hot climates. Energy Procedia 2017;109:138–45. https://doi.org/10.1016/j.egypro.2017.03.079.

[53] Reinholdt, L., Madsen, C., 2010. Heat recovery on CO2 systems in supermarkets. In: Proceedings of the 9th IIR Gustav Lorentzen Conference on Natural Refrigerants, 12th – 14th April; Sydney, Australia. ID: 143.

[54] Ringstad, K., Allouche, Y., Gullo, P., Ervik, Å., Banasiak, K., Hafner, A., 2020. A detailed review on CO2 two-phase ejector flow modeling. Thermal Science and Engineering Progress 20, 100647. doi: 10.1016/j.tsep.2020.100647.

[55] Sawalha S. Investigation of heat recovery in CO_2 trans-critical solution for supermarket refrigeration. Int J Refrig 2013;36(1):145–56. https://doi.org/10.1016/j.ijrefrig.2012.10.020.

[56] Schönenberger, J. Experience with R744 refrigerating systems and implemented multi ejectors and liquid overfeed. In: Proceedings of the 12th IIR Gustav Lorentzen Natural Working Fluids Conference, 21st – 24th August; Edinburgh, UK. ID: 1107.

[57] Singh S, Maiya PM, Hafner A, Banasiak K, Neksa P. Energy efficient multiejector CO_2 cooling system for high ambient temperature. Therm Sci Eng Prog 2020;19:100590. https://doi.org/10.1016/j.tsep.2020.100590.

[58] Sun Z, Wang C, Liang Y, Sun H, Liu S, Dai B. Theoretical study on a novel CO_2 Two-stage compression refrigeration system with parallel compression and solar absorption partial cascade refrigeration system. Energy Convers Manage 2020;204:112278. https://doi.org/10.1016/j.enconman.2019.112278.

[59] Tassou SA, Ge Y, Hadawey A, Marriott D. Energy consumption and conservation in food retailing. Appl Therm Eng 2011;31(2–3):147–56. https://doi.org/10.1016/j.applthermaleng.2010.08.023.

[60] Tsamos KM, Gullo P, Ge YT, IDew, Santosa, Tassou SA, et al. Performance investigation of the CO_2 gas cooler designs and its integration with the refrigeration system. Energy Procedia 2017;123:265–72. https://doi.org/10.1016/j.egypro.2017.07.237.

[61] Tsamos KM, Ge YT, Santosa IDMC, Tassou SA. Experimental investigation of gas cooler/condenser designs and effects on a CO_2 booster system. Appl Energy 2017;186(3):470–9. https://doi.org/10.1016/j.apenergy.2016.03.004.

[62] UNEP and IEA, 2020. Cooling Emissions and Policy Synthesis Report: Benefits of cooling efficiency and the Kigali Amendment. ISBN No: 978-92-807-3778-3 - Available at: <https://wedocs.unep.org/bitstream/handle/20.500.11822/33094/CoolRep.pdf?sequence=1&isAllowed=y> [accessed 08.01.2021].

[63] Xu XX, Chen GM, Tang LM, Zhu ZJ. Experimental investigation on performance of transcritical CO_2 heat pump system with ejector under optimum high-side pressure. Energy 2012;44(1):870–7. https://doi.org/10.1016/j.energy.2012.04.062.

[64] Yang J, Yu B, Chen J. Improved genetic algorithm based prediction of a CO_2 micro-channel gas-cooler against experimental data in automobile air conditioning system. Int J Refrig 2019;106:517–25. https://doi.org/10.1016/j.ijrefrig.2019.05.017.

[65] Zhu J, Elbel S. Experimental investigation into the influence of vortex control on transcritical R744 ejector and cycle performance. Appl Therm Eng 2020;164:114418. https://doi.org/10.1016/j.applthermaleng.2019.114418.